Current Biology 24, 1584–1595, July 21, 2014 ©2014 Elsevier Ltd All rights reserved http://dx.doi.org/10.1016/j.cub.2014.06.011

Article

Abdominal-B Neurons Control *Drosophila* Virgin Female Receptivity

Jennifer J. Bussell,[1] Nilay Yapici,[1] Stephen X. Zhang,[1,4] Barry J. Dickson,[2] and Leslie B. Vosshall[1,3,*]
[1]Laboratory of Neurogenetics and Behavior, The Rockefeller University, 1230 York Avenue, Box 63, New York, NY 10065, USA
[2]Janelia Farm Research Campus, Howard Hughes Medical Institute, 19700 Helix Drive, Ashburn, VA 20147, USA
[3]Howard Hughes Medical Institute

Summary

Background: Female sexual receptivity offers an excellent model for complex behavioral decisions. The female must parse her own reproductive state, the external environment, and male sensory cues to decide whether to copulate. In the fly *Drosophila melanogaster*, virgin female receptivity has received relatively little attention, and its neural circuitry and individual behavioral components remain unmapped. Using a genome-wide neuronal RNAi screen, we identify a subpopulation of neurons responsible for pausing, a novel behavioral aspect of virgin female receptivity characterized in this study.
Results: We show that *Abdominal-B* (*Abd-B*), a homeobox transcription factor, is required in developing neurons for high levels of virgin female receptivity. Silencing adult *Abd-B* neurons significantly decreased receptivity. We characterize two components of receptivity that are elicited in sexually mature females by male courtship: pausing and vaginal plate opening. Silencing *Abd-B* neurons decreased pausing but did not affect vaginal plate opening, demonstrating that these two components of female sexual behavior are functionally separable. Synthetic activation of *Abd-B* neurons increased pausing, but male courtship song alone was not sufficient to elicit this behavior.
Conclusions: Our results provide an entry point to the neural circuit controlling virgin female receptivity. The female integrates multiple sensory cues from the male to execute discrete motor programs prior to copulation. *Abd-B* neurons control pausing, a key aspect of female sexual receptivity, in response to male courtship.

Introduction

To choose their mates, male and female vinegar flies (*Drosophila melanogaster*) perform a duet of sexually dimorphic courtship behaviors that offers an excellent model for studying the neural circuitry of innate social behavior [1]. Male courtship is composed of a series of discrete and stereotyped motor programs such as following the female, producing courtship song using a single extended wing, tapping and licking her genitals, and finally, copulating [1]. The neural circuitry underlying several of these behavioral components has been identified and dissected [2]. In contrast, very little is known about how the female evaluates male courtship to decide whether to mate and how she executes that decision.

A female fly that engages in copulation is considered receptive to male courtship. Receptivity comprises the relative absence of obvious rejection behaviors, slowing down to allow the male to initiate copulation, and opening cuticular vaginal plates to allow access to the genitalia [3]. However, prior work on receptivity measured only mating rate, a metric that provides little insight into the discrete motor programs that females display in the context of courtship. Although classical genetic studies identified a region of the female brain [4] and genes required for receptivity [5–10], neurons with a clearly defined function specific to female behavior in courtship and mating have yet to be described.

Much of the effort to understand female receptivity has focused on its regulation. Female sexual maturity develops over the first few days after eclosion [11], and sexually immature adult females reject male courtship by running or jumping away and kicking and fluttering their wings [12]. After mating, female *Drosophila* temporarily switch into an unreceptive state in which they extrude the ovipositor to reject male courtship [12]. They also increase egg laying. This postmating response is triggered by Sex Peptide, which activates the Sex Peptide Receptor (*SPR*) [13] in a subset of female reproductive tract sensory neurons labeled by *pickpocket* (*ppk*), *fruitless* (*fru*), and *doublesex* (*dsx*) [14–16]. Although recent work has continued to identify neurons that function to coordinately regulate receptivity and egg-laying [14, 17], neurons with specific functions restricted to virgin mating behavior are still unknown.

Males present an array of sensory cues during courtship, including contact and volatile pheromones and courtship song. It is not known which sensory signals trigger individual components of receptivity and whether these components are coordinately or independently controlled by female neural circuitry. Song seems critical to the courtship process because males muted by having their wings removed have dramatically reduced mating success [18]. However, it remains unclear to what degree females integrate sensory input from courtship song with other male courtship cues and how song affects their behavior [19–21].

To expand the mechanistic understanding of *Drosophila* virgin female receptivity, we set out to characterize its component motor programs and identify neurons directly involved in this behavior. Using a genome-wide neuronal RNAi screen, we discovered a requirement for the homeobox (Hox) transcription factor *Abdominal-B* (*Abd-B*) in developing neurons for female receptivity. Adult *Abd-B-Gal4* neurons located in the abdominal ganglion and reproductive tract project locally within these areas and to higher brain centers. These neurons are functionally required for female receptivity and act to induce pausing in response to multiple male courtship cues. In addition to demonstrating a role for *Abd-B* in sex-specific behavior, our results identify a neuronal subset responsible for a discrete component of virgin female receptivity.

Results

An RNAi Screen Identifies Genes Required in Neurons for Female Reproductive Behaviors

We reasoned that genes and neural circuitry required for virgin female receptivity could be identified within hits of a

[4]Present address: Department of Neurobiology, Harvard Medical School, 220 Longwood Avenue, Boston, MA 02115, USA
*Correspondence: leslie.vosshall@rockefeller.edu

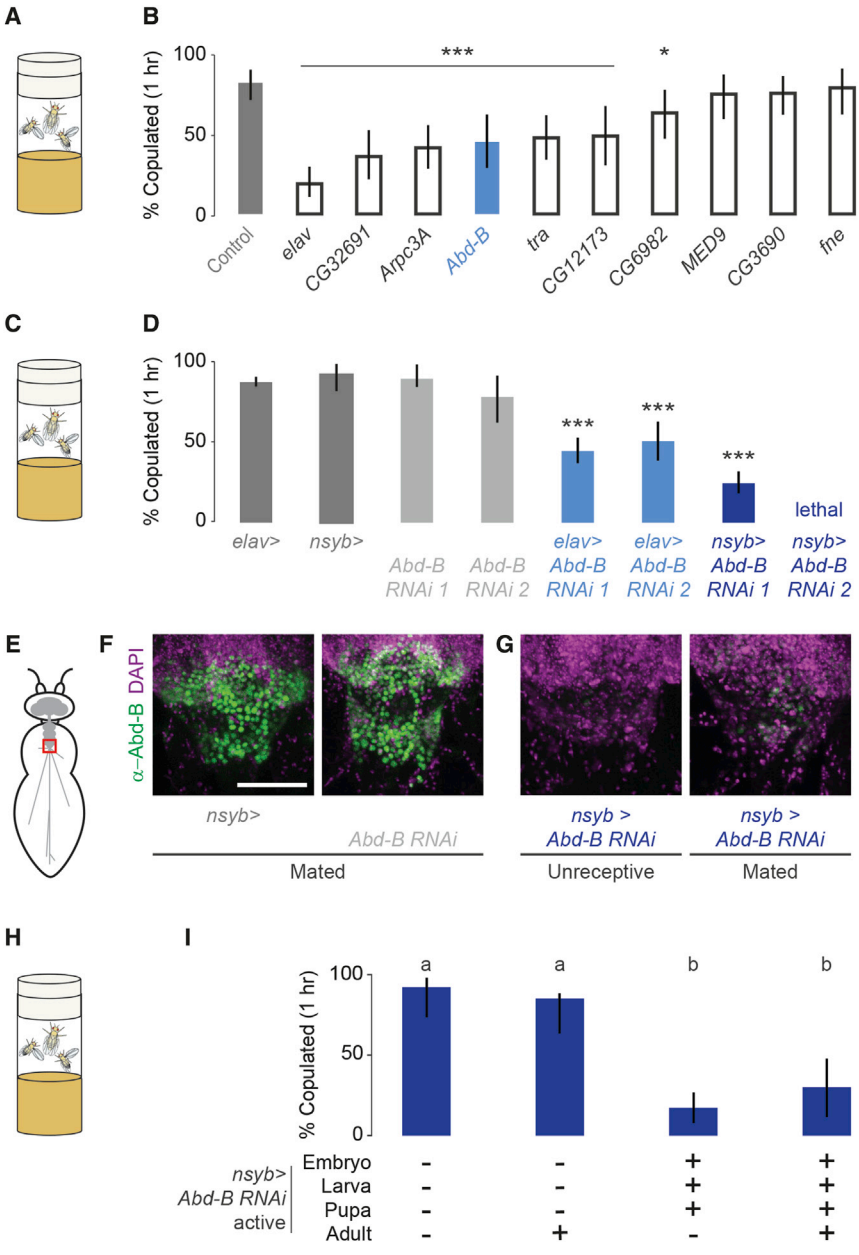

Figure 1. *Abd-B* Is Required in Neurons for Virgin Female Receptivity

(A, C, and H) Schematic of food vial mating assay with two males, shown here on either side of the female, with one wing extended.

(B and D) Receptivity of virgin females with *elav*- (B and D) or *nsyb*- (D) *Gal4*-driven RNAi against the indicated gene (***p < 0.0001 or *p < 0.005 compared to control [B] or ***p < 0.0001 compared to parental control [D]: pairwise Fisher's exact test with Bonferroni correction; mean and 95% confidence interval are shown, n = 30–300 (B), n = 30–273 [D]). *Abd-B* RNAi 1 is the original hairpin from the Vienna screen and was used in all other experiments. For unknown reasons, RNAi 2 when driven by *nsyb* was lethal, precluding further analysis.

(E) Schematic of the fly nervous system (gray) indicating the abdominal ganglion (red).

(F and G) Immunofluorescence of Abd-B (green) and nuclei (DAPI, magenta) in abdominal ganglia from females of the indicated genotype and mating status. Scale bar represents 50 μm.

(I) Receptivity of virgin females with *Abd-B* RNAi temporally restricted by shifts from 18°C to 30°C (***p < 0.0001, pairwise Fisher's exact test with Bonferroni correction; mean and 95% confidence interval are shown, n = 23–32). See also Figures S1 and S2.

genome-wide RNAi screen previously carried out to identify defects in female reproductive behaviors [13] (see Figure S1 available online). In this neuron-specific screen of the Vienna *Drosophila* RNAi library [22], males and females with pan-neuronal expression of each RNAi hairpin and Dicer2 to increase RNAi efficacy were allowed to mate, and egg-laying of female progeny was scored across 3 days (Figure S1A). Lines showing reduced egg-laying were rescreened twice to confirm the phenotype (Figure S1B), and 28 candidates were pursued further.

Reduced egg-laying in these strains could have been caused by deficits in female receptivity, the female postmating response, female fertility, or male mating success or fertility. To distinguish among these possible phenotypes, we carried out secondary assays for female receptivity, egg-laying, and remating (Figures S1C–1I). Of the 28 tested candidates, 10 showed decreased virgin female receptivity (Figure S1G), 10 showed decreased egg-laying without affecting receptivity (Figure S1H), and 3 were defective in postmating responses and showed both decreased egg-laying and increased remating (Figures S1H and S1I). Among the latter group was *SPR* [13]. Five candidates did not show a phenotype in secondary assays (*CG13243*, *mad2*, *sec15*, *Rack1*, and *CG12338*), perhaps because they affected male mating success or fertility.

Abd-B Is Required in Neurons for Female Receptivity

Seven of ten receptivity hits from Figure S1G showed a reduction in virgin female receptivity when rescreened in an assay pairing one virgin RNAi female with two wild-type (WT) males in a standard fly food vial for 1 hr (Figures 1A and 1B). Of these, we chose the Hox transcription factor *Abd-B* for further analysis because it has well-studied functions in specifying cell identity [23].

A second RNAi hairpin targeting *Abd-B* and a second pan-neuronal driver, *neuronal synaptobrevin (nsyb)-Gal4*, both showed decreases in receptivity (Figures 1C and 1D). Anti-Abd-B antibody staining [24] revealed many *Abd-B*-expressing neurons within the adult female abdominal ganglion of the ventral nerve cord (Figures 1E and 1F) and a smaller number of neurons within the reproductive tract (data not shown). *Abd-B* RNAi strongly reduced Abd-B immunofluorescence signal in the abdominal ganglion, in both unreceptive virgin females and the small fraction that mated (Figure 1G).

To assess whether *Abd-B* affects the development of the female receptivity circuit or is required for neuronal function

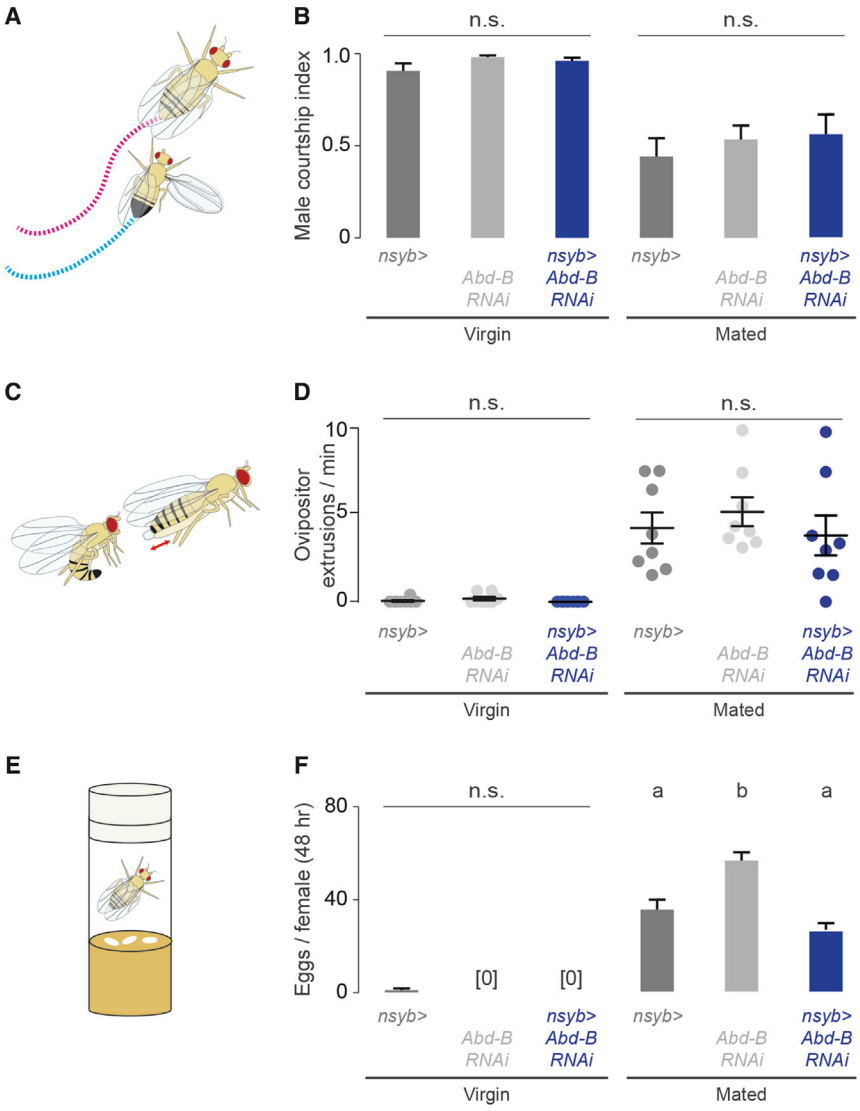

Figure 2. Neuronal *Abd-B* RNAi Does Not Induce the Postmating Response

(A, C, and E) Schematics of assays in (B), (D), (F).

(B) Courtship index of WT males during the first 5 min of courtship of a female of the indicated genotype and mating status (n.s., not significant, one-way ANOVA with Bonferroni correction, mean ± SEM, n = 8).

(D) Female ovipositor extrusion during assays in A (n.s., not significant, one-way ANOVA with Bonferroni correction, mean ± SEM, n = 8).

(F) Egg-laying during the first 48 hr after mating (n.s., not significant; bars labeled with different letters are significantly different: $p < 0.01$, one-way ANOVA with Bonferroni correction, mean ± SEM, n = 24–32).

in the adult, we temporally restricted *Abd-B* RNAi either to pre-adult stages or the adult by using *Gal80*^{ts}, a temperature-sensitive repressor of *Gal4* [25] (Figure S2). *Abd-B* RNAi active only during development caused a reduction in receptivity (Figures 1H and 1I), whereas RNAi active only in the adult showed no effect on receptivity (Figure 1I). We conclude that *Abd-B* plays a developmental role in forming the female receptivity circuit.

Neuronal Knockdown of *Abd-B* Does Not Induce the Postmating Response

We wished to learn whether the decreased copulation success of *Abd-B* RNAi virgin females was because they were unattractive to males or because they were prematurely switched into the unreceptive postmating state. Virgin *Abd-B* RNAi females tested in 1 cm plastic chambers with single WT males were as attractive to males as parental controls (Figures 2A and 2B). Mated, but not virgin, *Abd-B* RNAi females showed ovipositor extrusion (Figures 2C and 2D) and egg-laying (Figures 2E and 2F) and did not remate (data not shown). We conclude that the role of *Abd-B* in receptivity is independent of the postmating response.

Abd-B Receptivity Neurons Reside in the Abdominal Ganglion and Reproductive Tract

We accessed *Abd-B*-expressing neurons genetically with *Abd-B*^{LDN}, a *Gal4* insertion in the tethering element of the *Abd-B* promoter [26]. *Abd-B*^{LDN}-*Gal4* labeled 283 ± 10 (mean ± SEM, n = 3) cells in the adult female abdominal ganglion that were colabeled with antibody to Abd-B protein as well as a small number of colabeled cells in the reproductive tract (Figure 3A; data not shown).

To determine whether *Abd-B* RNAi restricted to *Abd-B*^{LDN}-*Gal4* positive neurons would yield receptivity defects, we limited *Abd-B*^{LDN} > *Abd-B* RNAi to neurons using the *nsyb* promoter. Briefly, we used the *lexA-lexAop* system [27] to express FLP recombinase in neurons under the control of the *nsyb* promoter and "flipped-out" ubiquitous *Gal80* [28] to relieve repression of *Gal4* only in neurons (see Supplemental Experimental Procedures for complete genotypes). Virgin females with *Abd-B* RNAi in *Abd-B*^{LDN}-*Gal4* neurons showed reduced receptivity (Figure 3B). Thus, *Abd-B*^{LDN}-*Gal4* labels a subset of *Abd-B* neurons important for female receptivity. Due to the expression of *Abd-B*^{LDN}-*Gal4* in nonneuronal tissue [26], using *Abd-B*^{LDN}-*Gal4* to drive *Abd-B* RNAi without this neuronal restriction produced females with malformed genitalia that were unable to copulate (data not shown).

To describe the anatomy of the *Abd-B* receptivity neurons, we examined the expression of nuclear (Figures 3C–3H) and membrane-bound (Figures 3I–3N) green fluorescent protein (GFP) driven by *Abd-B*^{LDN}-*Gal4*. *Abd-B*^{LDN}-*Gal4* showed restricted labeling of 280 ± 5 (mean ± SEM, n = 4) neurons in the abdominal ganglion (Figures 3D and 3E) and a small number of neurons within the reproductive tract and along the vaginal plates, as well as nonneuronal cells in the reproductive tract (Figures 3F–3H and arrowheads in Figures 3G and 3H). We did not observe any *Abd-B*^{LDN} neuronal cell bodies in the brain (Figure 3C).

Abd-B^{LDN} neurons project to several higher brain areas including the subesophageal zone, the ventrolateral neuropils, and the superior neuropils (Figure 3I), with extensive

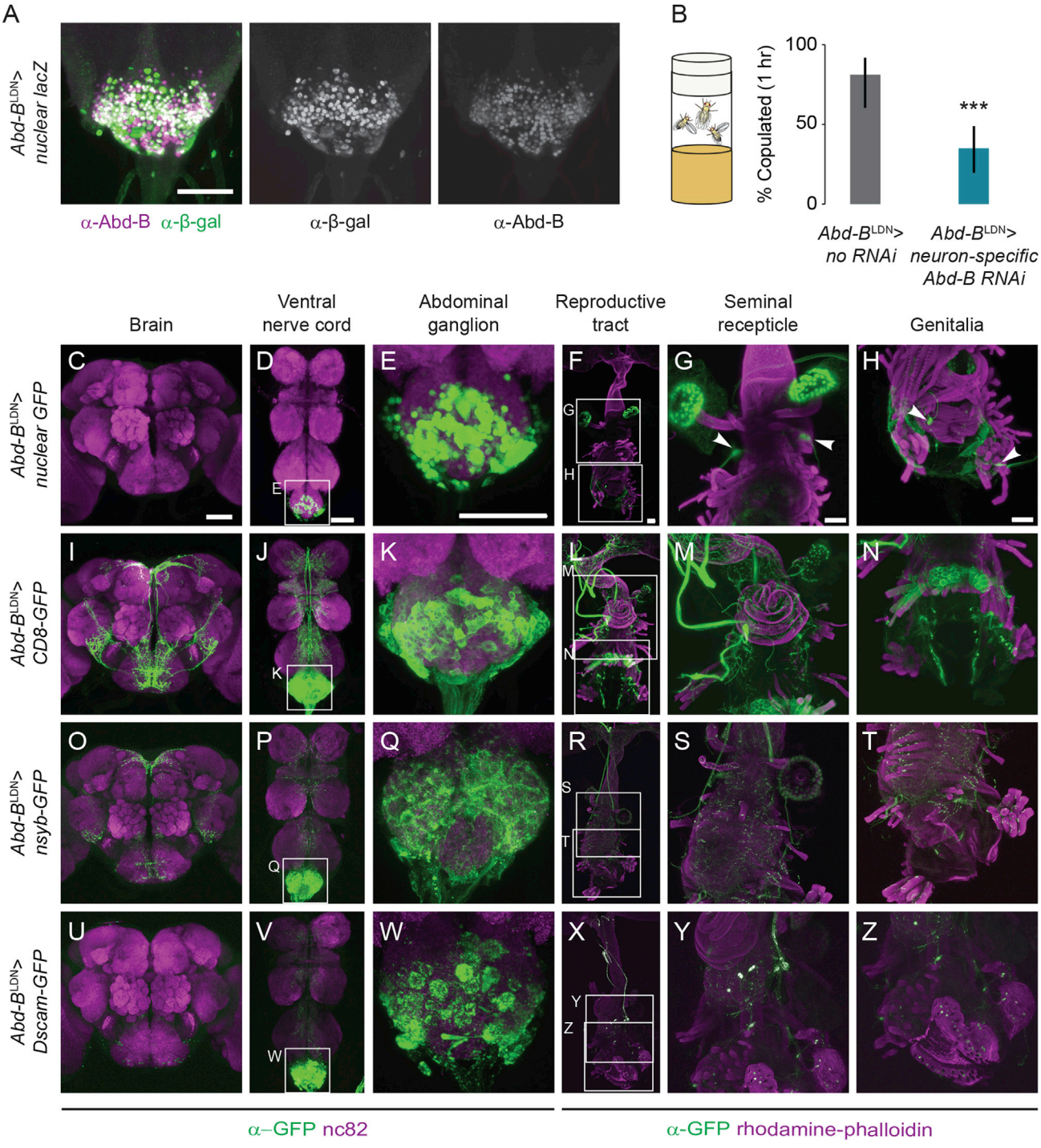

Figure 3. *Adb-B*^{LDN}*-Gal4* Labels *Abd-B* Receptivity Neurons in the Abdominal Ganglion and Reproductive Tract

(A) Colocalization of Abd-B (magenta) and nuclear lacZ (green) driven by *Abd-B*^{LDN}*-Gal4* in the virgin female abdominal ganglion. Scale bar represents 50 μm.

(B) Receptivity of virgin females with RNAi against *Abd-B* driven by *Abd-B*^{LDN}*-Gal4* and *UAS-Dcr2*, limited to neurons by *nsyb-lexA*, *lexAop-FLP*, and *tub-FRT-Gal80-FRT-STOP* (***$p < 0.001$, Fisher's exact test; mean and 95% confidence interval are shown, n = 16–40). See Supplemental Experimental Procedures for complete genotypes.

(C–Z) Immunofluorescence of GFP (green) and nc82 or rhodamine-phalloidin (magenta) in the indicated tissue in virgin females of the indicated genotype. Insets are separate z stacks at higher magnification of approximate areas indicated. Arrowheads in (G) and (H) indicate neuronal cell bodies. Scale bars represent 50 μm. See also Figure S3.

processes both within the abdominal ganglion and throughout the ventral nerve cord (Figures 3J and 3K). Within the female reproductive tract and terminalia, *Abd-B*^{LDN}*-Gal4*-labeled tissue and neuronal processes innervating the oviducts, uterus, muscles near the vaginal plates, and the vaginal bristles (Figures 3L–3N).

We used *Abd-B*^{LDN}-driven expression of GFP fused to *nsyb* (Figures 3O–3T) and *Dscam* (Figures 3U–3Z), enriched in axons and dendrites, respectively [29, 30], to examine the polarity of *Abd-B*^{LDN} neurons. Extensive *nsyb-GFP* labeling was found throughout the abdominal ganglion and ventral nerve cord, as well as in the subesophageal zone, ventrolateral neuropils, and superior neuropils in the brain (Figures 3O–3Q) and in the reproductive tract, particularly along muscle fibers, including those near the vaginal plates (Figures 3R–3T). *Dscam-GFP* labeling was absent in the brain but abundant in the abdominal ganglion of the ventral nerve cord (Figures 3U–3W). In the reproductive tract and terminalia, *Dscam-GFP* labeling was sparse but present along uterine and vaginal tissues (Figures 3X–3Z). Our interpretation of these staining patterns is that abdominal ganglion *Abd-B*^{LDN} neurons ascend to terminate in the ventral nerve cord and brain, with dendritic labeling enriched within the abdominal ganglion. They may also project axons within the abdominal ganglion itself and descend to innervate targets in the reproductive tract. Although *Abd-B*^{LDN} neuronal cell bodies reside within the reproductive tract, it was not possible to establish the polarity of projections of these neurons with these methods. We did not observe any differences in the projections of *Abd-B*^{LDN} neurons in the brain, ventral nerve cord, abdominal ganglion, or reproductive tract between 1-day-old immature virgin females and 4-day-old mature virgin females (Figure S3).

A Subset of *Abd-B* Neurons Is Functionally Required for Virgin Female Receptivity

Having established that *Abd-B* has a role in the development of the receptivity neural circuit, we asked whether *Abd-B*^{LDN} neurons are functionally important for receptivity in adult females. We used *UAS-shi*^{ts}, a dominant-negative variant of dynamin that transiently blocks chemical synaptic transmission at temperatures above 29°C [31], to silence *Abd-B*^{LDN} neurons during courtship. At the restrictive temperature, there was a selective decrease in receptivity only in virgin females carrying both *Abd-B*^{LDN} and *shi*^{ts} (Figure 4A). In females mated at the permissive temperature, acutely silencing *Abd-B*^{LDN} neurons 48 hr later modestly increased remating (Figure 4B), but not to the ~75% level found in mated *SPR* RNAi females (Figure S1I), which are deficient in the postmating response [13]. We used a second method of neuronal inactivation, *UAS-kir2.1* [32], to hyperpolarize *Abd-B*^{LDN} neurons chronically and again found decreased virgin receptivity (Figure 4C). *Abd-B*^{LDN} neurons are therefore functionally required for virgin female receptivity.

We carried out a series of experiments to restrict the expression of *Abd-B*^{LDN}*-Gal4* to a smaller subset of neurons that still decreased virgin receptivity using silencing with *kir2.1*. To confirm that *Abd-B*^{LDN} > *kir2.1* is required in neurons for the receptivity phenotype, we used *elav-Gal80* [15] to suppress *Abd-B*^{LDN}*-Gal4* activation in neurons (Figure S4A) and rescued receptivity as expected (Figure 4C). *teashirt (tsh)-Gal80* is expressed in a large subset of ventral nerve cord cells [33] and suppressed *Gal4* activation in approximately half of the *Abd-B*^{LDN} neurons, leaving 142 ± 2 (mean ± SEM, n = 4) neurons in the abdominal ganglion, as well as those in the reproductive tract (Figures S4B and S4C). Silencing only this subset of *Abd-B*^{LDN} neurons in the presence of *tsh-Gal80* was sufficient to reduce virgin female receptivity (Figure 4C).

Projections of *Abd-B*^{LDN} neurons are found near the oviposition, uterus, and vaginal plates. To ask whether *Abd-B*^{LDN} receptivity defects were due to function in descending motor neurons, we created a *Gal80* line using the *Drosophila* vesicular glutamate transporter (*VGlut*) promoter [34] to suppress *Abd-B*^{LDN}*-Gal4* activation in motor neurons. *VGlut-Gal80* removed the muscle-innervating *Abd-B*^{LDN}*-Gal4* projections in the female reproductive tract (Figures S4D and S4E), but receptivity remained strongly impaired in this strain, suggesting that motor neurons are not major contributors to the receptivity phenotype (Figure 4C).

We next asked whether *ppk* sensory neurons in the reproductive tract involved in postmating female behaviors [15, 16] contributed to our receptivity phenotype. Using *ppk-Gal80* [15, 16] (Figures S4F and S4G), we found no effect on the reduction in virgin female receptivity with *Abd-B*^{LDN} > *kir2.1* (Figure 4C). Although these data suggest that neither motor neurons nor the *ppk*-expressing sensory neurons are major contributors to the receptivity phenotype, we cannot rule out a contribution from non-*ppk*-positive and non-*VGlut*-positive neurons in the reproductive tract and genitalia.

In addition to the *ppk* neurons, neurons labeled by *dsx-Gal4* have been shown to play a role in female mating behavior [35]. Specifically, silencing a subset of *dsx-Gal4* neurons in the abdominal ganglion by intersection with an enhancer-trap *FLP* recombinase line (*Et*^{FLP250}) blocks the postmating response and increases mated female receptivity [14]. Because this neuronal subset is the intersection of *Et*^{FLP250} and *dsx-Gal4*, if it contributes to the *Abd-B*^{LDN} receptivity phenotype, *Et*^{FLP250} should intersect a subset of *Abd-B*^{LDN} neurons functionally important for virgin female receptivity. We therefore carried out intersectional neuronal silencing experiments using *UAS-FRT-STOP-FRT-kir2.1*. In control experiments, we showed that intersectional silencing of all *Abd-B*^{LDN} neurons using *nsyb-lexA, lexAop-FLP* (*neuronal FLP*) reproduced the receptivity phenotype (Figure 4D). Although *Et*^{FLP250} does intersect a population of *Abd-B*^{LDN} neurons (Figures 4E–4J), silencing this subset had no effect on virgin female receptivity (Figure 4D). Thus *Abd-B*^{LDN} receptivity neurons comprise neither of the previously described *ppk* or *dsx*∩*Et*^{FLP250} neuronal subsets contributing to female-specific behaviors.

Given the central role of *fruitless*-labeled neurons in *Drosophila* courtship behavior [2] and the fact that silencing *fru-Gal4*-labeled neurons in females decreases receptivity [36], we tested whether *Abd-B*^{LDN}*-Gal4* expression overlaps with *fru*. We intersected *Abd-B*^{LDN}*-Gal4* with *fru* neurons using *fru-FLP* [2], and although there is a *fru* subset of *Abd-B*^{LDN} neurons (Figures 4K–4P), this subset does not contribute to the *Abd-B*^{LDN} receptivity phenotype (Figure 4D).

We also asked whether *Abd-B*^{LDN} neurons play a role in male sexual behavior. *Abd-B*^{LDN}*-Gal4* labels neurons in the male ventral nerve cord, as well as neurons in the male reproductive tract (Figures S5A–S5J). However, these neurons are not functionally required for male courtship or copulation (Figure S5K; data not shown). Males have approximately the same number of *Abd-B*^{LDN} ventral nerve cord neurons as females (280 ± 2, mean ± SEM, n = 3), but there is increased labeling in the flange within the subesophageal zone and the lateral protocerebrum in males and decreased labeling of projections in the superior medial protocerebrum (arrowheads in Figure S5A) relative to females.

Silencing *Abd-B* Neurons Decreases Pausing during Courtship

To determine the specific role of *Abd-B*^{LDN} neurons in female receptivity, we examined the behavior of females with silenced

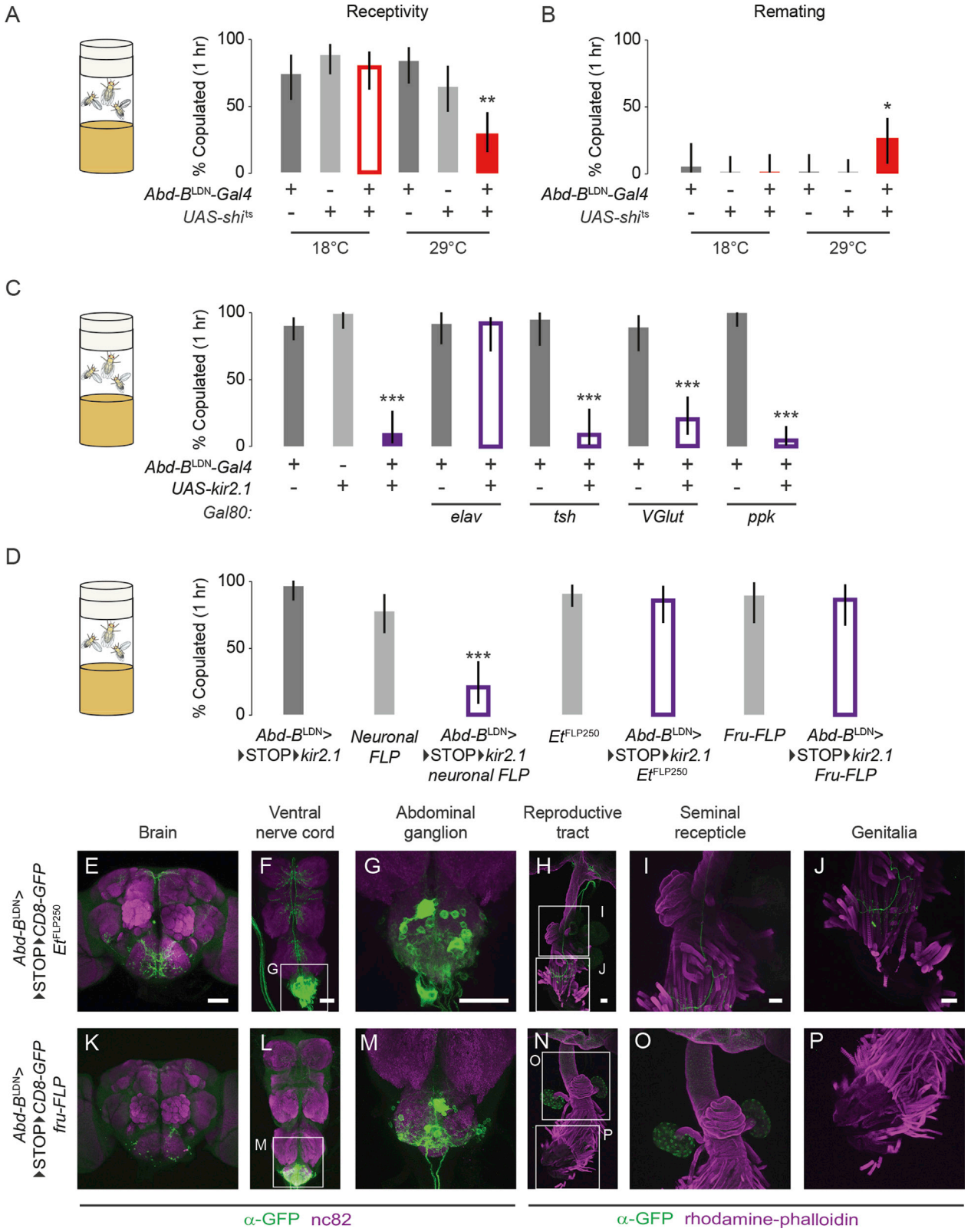

Figure 4. *Abd-B*^{LDN} Neurons Are Functionally Required for Virgin Female Receptivity

(A and B) Temperature-shift receptivity of virgin females (A) or females 48 hr after mating (B).

(C and D) Receptivity of virgin females. In (A)–(D), *p < 0.05, **p < 0.01, ***p < 0.001 compared to parental controls (at the same temperature in A and B), Fisher's exact test; mean and 95% confidence interval are shown. Sample sizes are as follows: n = 33–40 (A), n = 23–35 (B), n = 20–59 (C), n = 29–56 (D).

(E–P) Immunofluorescence of GFP (green) and nc82 or rhodamine-phalloidin (magenta) in the indicated tissue in virgin females of the indicated genotype. Insets are separate z stacks at higher magnification of approximate areas indicated. Scale bars represent 50 μm. See also Figures S4 and S5.

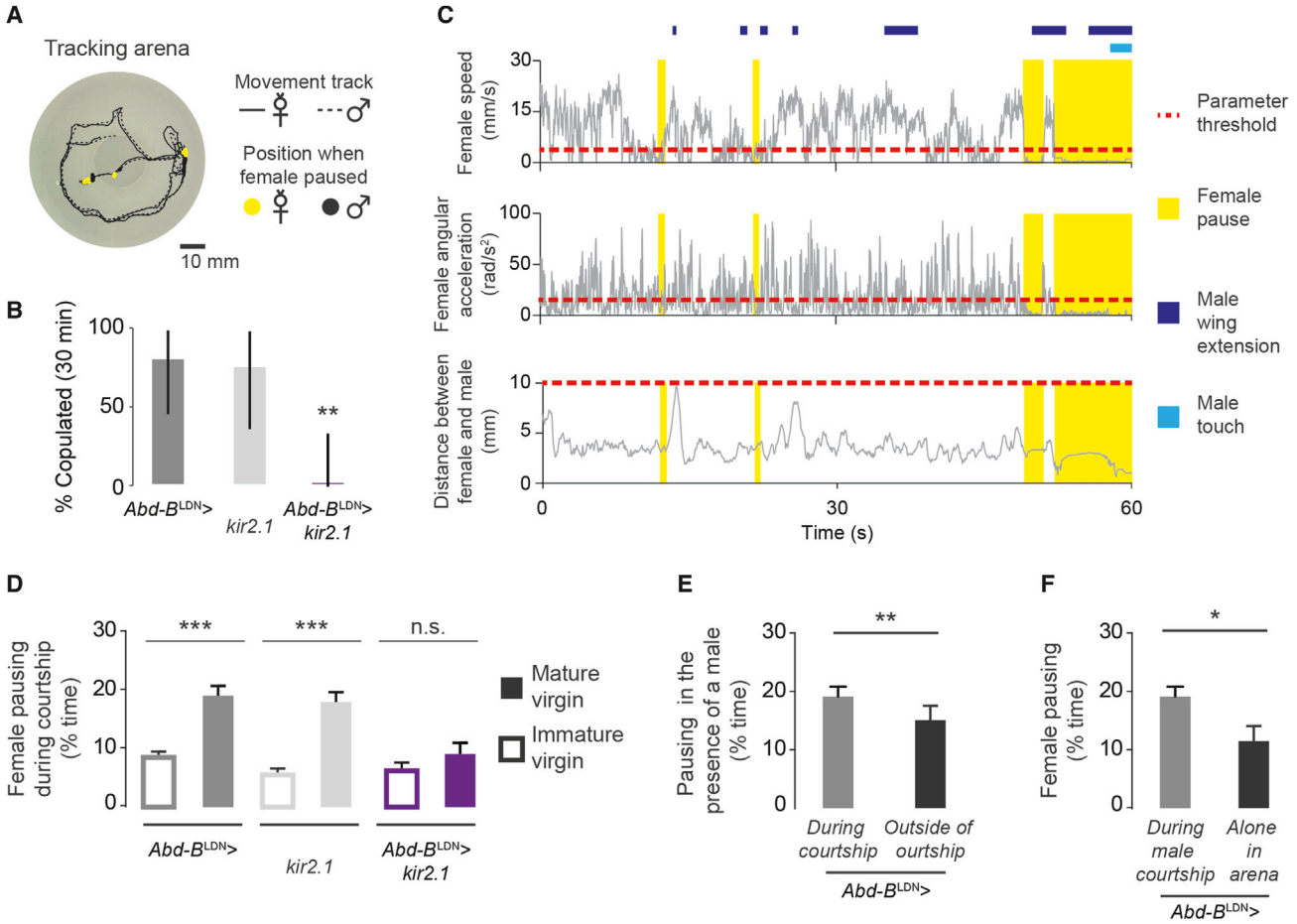

Figure 5. Silencing *Abd-B*^{LDN} Neurons Decreases Pausing during Courtship

(A) Tracking arena with fly positions during the last 60 s before copulation between *Abd-B*^{LDN}*-Gal4* mature virgin female and WT male.

(B) Receptivity of virgin females in the tracking arena (**p < 0.01 compared to parental controls, Fisher's exact test; mean and 95% confidence interval are shown, n = 8–10).

(C) Per-frame parameters calculated from tracks in (A).

(D) Female pausing during courtship (Student's t test, mean ± SEM, n = 8–10, ***p < 0.001).

(E) Female pausing in the presence of a male (Student's t test, mean ± SEM, n = 10, **p < 0.01).

(F) Female pausing (Student's t test, mean ± SEM, n = 8–10, *p < 0.05). See also Figure S6 and Movies S1 and S2.

Abd-B^{LDN} neurons during courtship. We compared sexually mature virgin females to immature 1-day-old females, which are reported to run and jump away to avoid male courtship [12]. We first quantified two abdominal behaviors: vaginal plate opening and ovipositor extrusion (Figures S6C–S6F; Movie S1). While sexually immature virgin females did not open the vaginal plates, mature virgin females periodically opened their vaginal plates during courtship (Figure S6D). The transition to intermittent vaginal plate opening during courtship was intact in virgin females with silenced *Abd-B*^{LDN} neurons, and we conclude that *Abd-B*^{LDN} neurons are not functionally required for vaginal plate opening. Neither immature 1-day-old nor mature 4-day-old *Abd-B*^{LDN} > *kir2.1* females showed significant ovipositor extrusion (Figure S6F).

To quantify slowing down during courtship, we tracked the movement of pairs of male and female flies using Ctrax software [37] (Figure 5A) in a large arena in which *Abd-B*^{LDN} > *kir2.1* females also showed a strong receptivity defect (Figure 5B). Female walking speed during courtship did not differ with sexual maturity (Figure S6I), suggesting that receptive females do not generally slow their movement during courtship. Mature virgin *Abd-B*^{LDN} > *kir2.1* females walked at the same speed as control females during courtship (Figure S6I).

Instead, we identified periods in which the female "paused" during courtship (Figures 5C and 5D; Movie S2). The percent of time spent pausing was nearly doubled in control receptive virgin females compared to unreceptive immature virgins (Figure 5D). Mature virgins paused more when being courted by a male than during periods when the male was present, but not courting (Figure 5E), and they paused more during courtship than when in the arena alone (Figure 5F). Taken together, these data suggest that increased pausing is a specific hallmark of female receptivity and not a more generalized developmental motor change. Mature virgin *Abd-B*^{LDN} > *kir2.1* females paused very little and were indistinguishable in this response from immature virgins (Figure 5D). Thus, *Abd-B*^{LDN} neurons are functionally required for the pausing component of receptivity.

Despite the decreased pausing of *Abd-B*^{LDN} > *kir2.1* females, males attempted copulation as much with *Abd-B*^{LDN} > *kir2.1* females as parental controls (Figures S6A and S6B) and displayed high levels of courtship as measured by

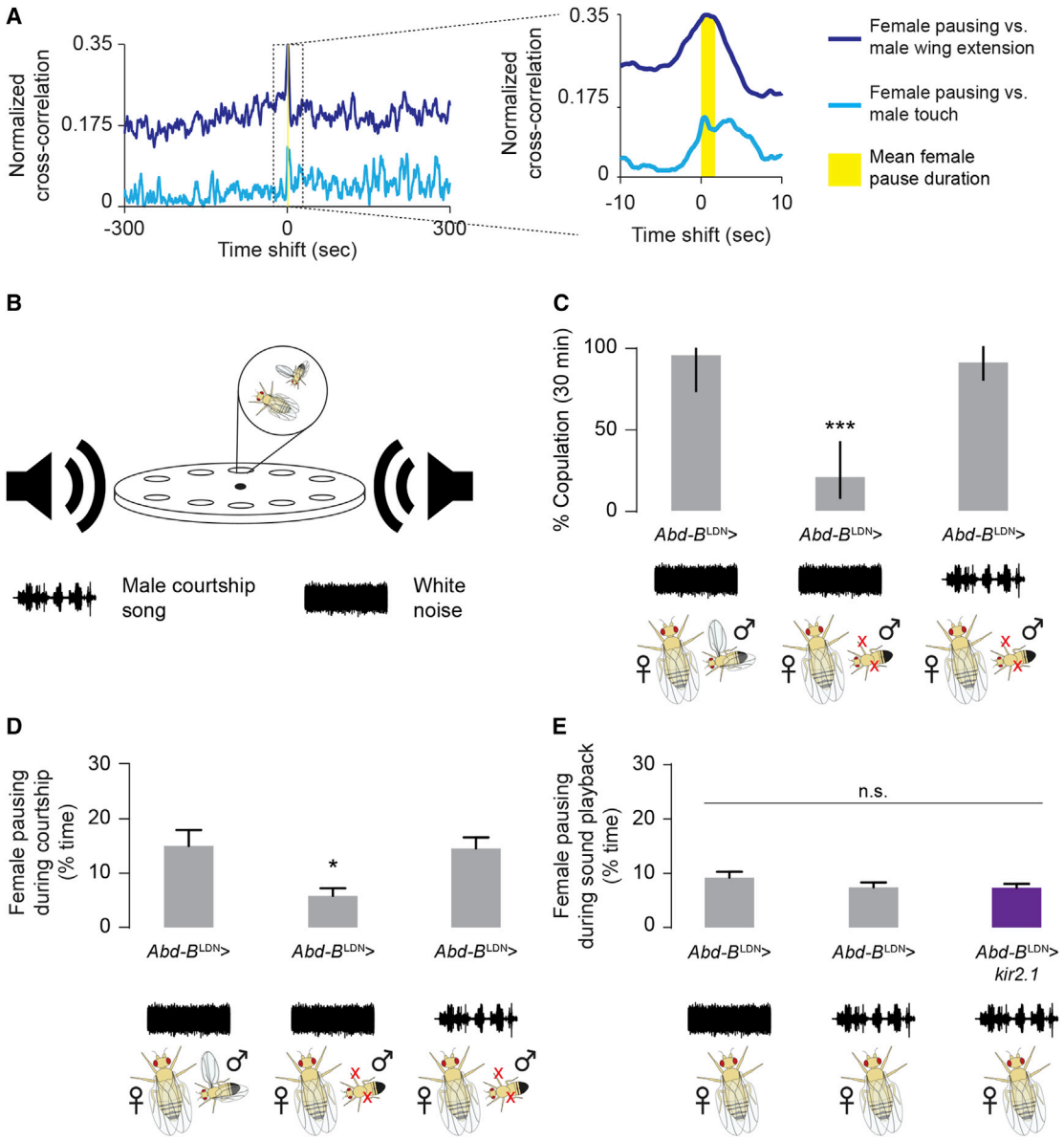

Figure 6. Pausing Is a Response to Multiple Male Courtship Cues

(A) Cross-correlation between female pausing and male wing extension or male touch during courtship tracking assays with *Abd-B*^{LDN}*-Gal4* mature virgin females and wild-type males (n = 5).

(B) Schematic of sound playback assay.

(C) Receptivity of *Abd-B*^{LDN}*-Gal4* mature virgin females during sound playback with WT males with and without wings as indicated (***p < 0.001, Fisher's exact test; mean and 95% confidence interval are shown, n = 23–24.

(D and E) Pausing of mature virgin females with WT males with and without wings as indicated (D) or in the absence of a male (E) during sound playback (n.s., not significant, *p < 0.05, one-way ANOVA with Bonferroni correction, mean ± SEM; n = 6–7 [D], n = 22–23 [E]).

courtship index (Figures S6G and S6H). Additionally, *Abd-B*^{LDN} > *kir2.1* females did not run away from courting males: the distance between these females and courting males was the same as parental controls (Figures S6J).

Pausing Is a Response to Multiple Male Courtship Cues

To understand more about the regulation of female pausing by male sensory cues, we performed a cross-correlation analysis of female pausing during courtship and male touch and wing extension, which served as a proxy for courtship song (Figure 6A). Both of these behaviors were weakly correlated with female pausing. The normalized cross-correlation of wing extension was stronger than that of touch and was centered at zero time shift, suggesting that courtship song might provide sensory input to the neuronal circuit controlling female pausing.

To test this, we set up an assay to play recorded courtship song while tracking fly movement (Figure 6B). In control experiments, we determined that white noise sound playback did not affect female receptivity and that muting males by removing their wings decreased female receptivity (Figure 6C). As previously reported [38], playback of recorded

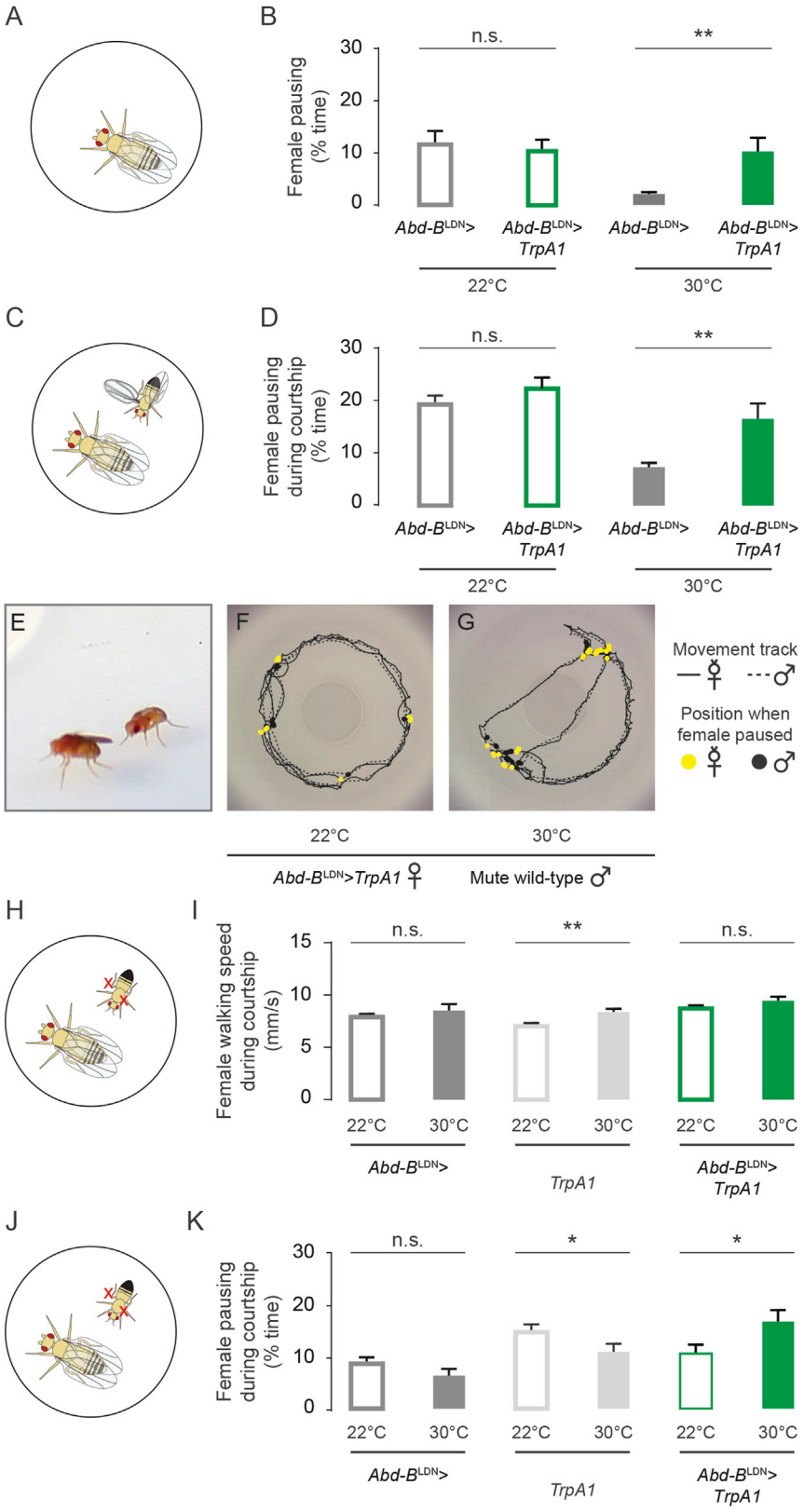

Figure 7. Activating *Abd-B* Neurons Induces Pausing

(A) Schematic of assay in (B).

(B) Temperature-shifted pausing of mature virgin females in the absence of a male (n.s., not significant, **p < 0.01, Student's t test, mean ± SEM, n = 7–10).

(C) Schematic of assay in (D).

(D) Temperature-shifted pausing of mature virgin females during courtship from WT males (n.s., not significant, **p < 0.01, Student's t test, mean ± SEM, n = 7–11).

(E) Video frame of *Abd-B*^{LDN}*-Gal4* mature virgin female and WT male without wings in tracking arena.

(F and G) Tracked fly positions during the fourth min of courtship between *Abd-B*^{LDN}*-Gal4* > *TrpA1* mature virgin female and WT male without wings at 22°C (F) or 30°C (G).

(H) Schematic of assay in (I).

(I) Temperature-shifted female speed excluding frames classified as pausing during courtship from a male without wings (n.s., not significant, **p < 0.01, Student's t test, mean ± SEM, n = 12–16).

(J) Schematic of assay in (K).

(K) Temperature-shifted pausing of virgin females during courtship from males without wings (n.s., not significant, *p < 0.05, Student's t test, mean ± SEM, n = 12–16). See also Figure S7 and Movie S2.

courtship song rescued female receptivity with mute males (Figure 6C).

We next asked whether female pausing correlated with the effect of courtship song on receptivity and found that pausing was decreased when mute males were paired with white noise (Figure 6D). Pausing was rescued by playback of song during courtship with a mute male (Figure 6D). However, playback of recorded courtship song to females without a male present was not sufficient to increase pausing whether or not their *Abd-B*^{LDN} neurons were silenced (Figure 6E). From these data, we conclude that pausing requires the integration of song with other male sensory cues during courtship.

Activating *Abd-B* Neurons Induces Pausing

To determine whether the activity of *Abd-B*^{LDN} neurons induces pausing, we synthetically activated them by expressing *Drosophila TrpA1*, a heat-activated nonselective cation channel [39]. Isolated females were assayed in our tracking arena (schematized in Figure 7A) at control temperatures or elevated temperatures that activated *TrpA1*. Although the higher temperature itself decreased pausing in control animals ($p < 0.001$, Student's t test, n = 8–10), activation of *Abd-B*^{LDN} neurons counteracted this effect (Figure 7B). *TrpA1* activation of *Abd-B*^{LDN} neurons also increased pausing relative to the elevated-temperature control in the context of courtship with a WT male (Figures 7C and 7D). Thus, activation of *Abd-B*^{LDN} neurons is sufficient to increase pausing in both the presence

and absence of male courtship. However, females with *Abd-B*^{LDN} > *TrpA1* activation did not copulate (Figures S7A and S7B), perhaps because this manipulation caused the vaginal plates to be locked in a spread-open position and unable to open and close (Figures S7C and S7D; Movie S1). Although *Abd-B*^{LDN} neurons are not required for vaginal plate opening during courtship, there is at least a subset of *Abd-B*^{LDN} neurons that can affect the movement of the vaginal plates.

We sought to determine whether activation of *Abd-B*^{LDN} neurons could compensate for the lack of song during courtship with a mute male (Figures 7E–7G). *TrpA1* activation had no effect on female walking speed (Figures 7H and 7I) and did not render the animals stationary, suggesting that *Abd-B*^{LDN} neurons act within a receptivity pausing circuit rather than a more general locomotion control pathway. Activating *Abd-B*^{LDN} neurons was sufficient to increase pausing during courtship with a mute male (Figures 7J and 7K). Thus, we conclude that *Abd-B*^{LDN} neurons are both necessary and sufficient for the female pausing response to male courtship.

Discussion

Female receptivity is a complex behavior comprising multiple motor programs and requiring the integration of sensory cues across several modalities. Nevertheless, *Drosophila* mating behavior is innate, and receptivity is likely controlled by hard-wired neural circuits. We identified seven candidate genetic markers of receptivity neurons by using a neuronal RNAi screen. Our data suggest a central role for one of these, the transcription factor *Abd-B*, in forming a neural circuit that functions in receptivity.

We have refined the behavioral components of receptivity beyond mere copulation acceptance. We show that vaginal plate opening occurs throughout courtship and depends on sexual maturity. We also attribute the historically noted slowing down of receptive females to punctuated bouts of pausing during courtship rather than decreased walking speed. Pausing behavior is specific to female receptivity: it is decreased in both unreceptive females and in mature virgin females not being actively courted by a male. The increased level of pausing associated with receptivity requires the integration of multiple sensory inputs, including song, from a courting male. *Abd-B*^{LDN} neuronal activity is both necessary for this pausing response and sufficient to induce it, thus establishing direct function of these neurons within the receptivity circuit.

How do *Abd-B* neurons control pausing? The *Abd-B*^{LDN} neurons important for receptivity are not themselves motor neurons, and females with silenced *Abd-B*^{LDN} neurons are not generally deficient in movement or posture. This suggests that *Abd-B*^{LDN} neurons play a role downstream of the sensation of individual male courtship sensory inputs but upstream of motor output. The abdominal ganglion is emerging as a potential locus coordinating female-specific behavior [14, 40, 41], and *Abd-B*^{LDN} neurons there are well-positioned to interact with other neurons involved in female behavior, including the postmating response. These neurons could therefore potentially function to integrate male courtship cues and internal inputs and promote pausing.

Silencing *Abd-B*^{LDN} neurons affects pausing, but not vaginal plate opening, which demonstrates that it is possible to uncouple these two aspects of receptivity. However, activation of *Abd-B*^{LDN} neurons affects both pausing and the movement of the vaginal plates. It is therefore possible that *Abd-B*^{LDN} neurons, or subsets within them, function in both of these aspects of receptivity. There are likely to be additional circuit components involved in plate opening that might be able to act redundantly in the absence of *Abd-B*^{LDN} neurons, and the involvement of additional neurons in the control of the vaginal plates is consistent with the fact that *Abd-B*^{LDN} activation does not induce periodic vaginal plate opening but rather locks the plates in the open position. How the receptivity circuitry coordinates vaginal plate opening with pausing and male copulation attempts remains unknown. *Abd-B*^{LDN} neurons provide an important entry point to dissect the two female motor programs. We observed that vaginal plate opening occurs both while the female is moving and while she is stationary. Female movement has been shown to provide feedback to the male during courtship [42], and it could be that pausing provides an important connection between the sexes within the context of the courtship duet.

Abd-B is required in neurons during development for females to become highly receptive to male courtship. How does the Abd-B protein affect the receptivity circuitry? Our *Abd-B*^{LDN} > *Abd-B* RNAi experiments show that *Abd-B*^{LDN}-*Gal4* labels the neurons in which Abd-B functions during development to affect receptivity. However, we note that it is possible that these developmental *Abd-B*^{LDN} neurons are not identical to the adult *Abd-B*^{LDN} neurons we show to function in receptivity. In developing neuroblasts, *Abd-B* can have different, even opposing, functions, promoting cell death or promoting a particular cell fate or repressing it, depending on neuroblast identity and context [23]. In our *Abd-B*^{LDN} > *Abd-B* RNAi experiments, we did not observe any obvious changes in either the number or projections of *Abd-B*^{LDN} neurons in the adult, but this does not exclude the possibility of subtle anatomical changes or changes in cell identity.

Finally, we note that modularity in the control of complex innate behavior has been found across a variety of species and systems. From flies to mice, both aggression and mating are controlled by eliciting different modules in a sexually dimorphic way [2, 43, 44]. Thus, female fly receptivity fits into a larger pattern of sex-specific control of innate behavioral components.

Experimental Procedures

Fly Stocks

Flies were maintained on conventional cornmeal-agar-molasses medium under a 12 hr light: 12 hr dark cycle (lights on 9 a.m.) at 25°C and 60% relative humidity, unless otherwise indicated. Canton-S was used as WT. Sources of all fly strains and detailed genotypes can be found in the Supplemental Experimental Procedures.

Transgenic Flies

VGlut-Gal80 was generated by PCR amplification of the 5.3 kb *dVGlut* promoter fragment from the *pC56-Kan dVGlut5* vector (kind gift of Richard Daniels, University of Wisconsin) [34] and cloned via the Gateway system (Life Technologies) into the *pBPGAL80Uw-6* vector [45]. The *VGlut-Gal80* vector is available at AddGene (Plasmid #52555). Transgenic flies (strain available as Bloomington Stock #55847) were generated with standard methods (Genetic Services).

Immunostaining and Microscopy

Tissue was dissected in 4°C phosphate-buffered saline (PBS) (Ca^{+2}, Mg^{+2} free; Lonza BioWhittaker CAT#17-517Q), fixed in 4% paraformaldehyde in PBS for 20 min at 23°C, washed 4–6 times over 2 hr in PBT (PBS and 0.1% Triton X-100), and blocked for 1 hr in PBT + 5% goat serum at 23°C before incubation with primary antibodies diluted in PBT + 5% goat serum for 48 hr at 4°C. Samples were washed 4–6 times over 2 hr in PBT at 23°C before application of secondary antibodies for 48 hr at 4°C. Samples were washed again 4–6 times over 2 hr in PBT and mounted in VectaShield

containing DAPI (Vector Labs) on glass slides with bridging coverslips. Confocal sections were acquired with a Zeiss LSM510 confocal microscope. For details on antibodies used, see the Supplemental Experimental Procedures.

RNAi Screen

The genome-wide neuronal RNAi screen was carried out by N.Y. in the laboratory of B.J.D. at the Research Institute of Molecular Pathology (IMP) in 2005–2008 with the VDRC RNAi library [22]. Detailed information on the RNAi screen is in Supplemental Experimental Procedures.

Behavioral Assays

These assays were carried out by J.J.B. in the laboratory of L.B.V. at The Rockefeller University in 2009–2014. All assays were performed at ZT3-9, and all genotypes and conditions were tested on at least three different occasions. Virgin females were collected within 6 hr of eclosion, group-housed without males, and tested at 4–6 days old. Immature virgin females were tested at 24 hr posteclosion. Mated females were individually observed copulating with 1 of 2 males in a food vial at 4–5 days old and tested 48 hr later. WT Canton-S males were collected 0–2 days after eclosion and were group-housed away from females for 3–7 days. Temperature-shifted experiments were carried out in incubators (Insect model BC26-IN, BioCold Environmental).

Copulation Assays

Single females were gently aspirated into standard fly food vials containing two WT males at 23°C. Individual pairs were visually scored for copulation at 5, 10, 15, 30, 45, and 60 min to determine the percent copulated during 1 hr.

Temporally Restricted RNAi

tub-Gal80^{ts} [25] crosses were reared at either 18°C or 30°C. Virgin females were collected at eclosion and then group-housed away from males for 4 days at either 18°C or 30°C before being tested for receptivity at 23°C or dissected.

Male Courtship Index

Courtship index was defined as the proportion of time the male followed and oriented toward the female within 5 min of courtship initiation, marked by the initial orientation toward and following of the female. Male courtship index in Figure 2B was scored from the same videos as ovipositor extrusion in Figure 2D.

Vaginal Plate Opening and Ovipositor Extrusion

Individual females were placed in one of eight 1 cm circular plastic chambers in a courtship wheel with a WT male and filmed for 15 min. To allow visualization of vaginal plate opening, we recorded uncompressed image sequences at 1,600 × 1,200 pixels and 30 frames per s and less than 10 ms exposure directly to disk with a Grasshopper-2 Firewire camera (Point Grey Research) with an Infinimite Alpha lens and 2X magnifier (Infinity Optics) using Streampix 5 (Norpix). Lighting was provided by angled low-flicker fluorescent lights (Coherent) and adjustable fiber optic lights from a dissecting microscope. Instances of vaginal plate opening and ovipositor extrusion were scored blind to genotype and mating status from frame-by-frame playback during the first 5 min of courtship or until copulation if it occurred within 5 min. Courtship initiation was defined as the male orienting toward and beginning to follow the female. Rare trials with fewer than 30 s of total courtship were discarded.

Egg Laying

Individual virgin females were observed to mate with a WT male in a fly food vial and then transferred singly into food vials at 25°C, 60% relative humidity, 12 hr light: 12 hr dark and allowed to lay eggs for 24 hr. Adults were then transferred to a fresh vial and allowed to lay for another 24 hr. The number of eggs was counted at the end of each 24 hr period to determine total eggs laid per female in 48 hr.

Acute Neuronal Silencing

Flies for *UAS-shi*^{ts} [31] silencing experiments were raised at 18°C and shifted to 18°C or 29°C 30 min prior to assays. Food vials were placed at 18°C or 29°C for 2 hr prior to assays to reach the appropriate temperature.

Movement Tracking

Fly movement in two dimensions was tracked during courtship in a custom 70 mm circular arena with sloping sides and a removable level center modified from published designs [46]. The arena was made of opaque white Delrin plastic (McMaster-Carr) custom-machined to uniform thickness to allow even backlighting from a light board (Smith-Victor Corporation CAT#A-5A) and topped with a piece of Plexiglas with a small hole for introducing flies. Plans are available upon request. Video was recorded with a consumer camcorder (Canon HFS20) mounted above the arena in an incubator at 60% relative humidity with the lights on. Movement was tracked with Ctrax open source software [37]. Details are in the Supplemental Experimental Procedures.

Sound Playback

Recordings were played with Audacity software (http://audacity.sourceforge.net/) from a laptop computer on AX210 computer speakers (Dell). The two speakers were placed on opposite sides of an 8-chamber Plexiglass wheel (12 cm diameter) with mesh bottom. The song file was composed of 4 repeats of an approximately 20 min section of WT Canton-S male courtship song [47]. Intensity-matched white noise with amplitude 0.8 was generated with Audacity's noise-generation function.

Mute Males with Wings Removed

To generate mute males, we lightly anesthetized 4–5 day old males with carbon dioxide and removed their wings as close to the base as possible with dissecting scissors. Operated males were allowed to recover as a group for at least 24 hr at 25°C, 60% relative humidity, and were used within 72 hr of wing removal.

Neuronal Activation

Flies for *UAS-TrpA1* activation experiments were raised at 22°C. Assays were conducted at 22°C or 30°C, with flies introduced to the appropriate temperature at the start of assays. The tracking arena was placed at 22°C or 30°C for 2 hr prior to assays to reach the appropriate temperature.

Statistical Analysis

Statistical analysis was performed with GraphPad Prism Software version 6.01 (GraphPad Software).

Supplemental Information

Supplemental Information includes seven figures, Supplemental Experimental Procedures, and two movies and can be found with this article online at http://dx.doi.org/10.1016/j.cub.2014.06.011.

Author Contributions

J.J.B. designed and carried out all the experiments in the paper except for Figure S1, which was carried out by N.Y. under the supervision of B.J.D. S.X.Z. constructed the *VGlut-Gal80* vector and developed the initial pausing identification Matlab script. J.J.B. and L.B.V. together composed the figures and wrote the paper.

Acknowledgments

We thank Cori Bargmann, Vanessa Ruta, Gaby Maimon, and members of the Vosshall Laboratory for discussion and comments on the manuscript; Carlos Ribeiro for his collaborative efforts on the RNAi screen; Mala Murthy, David Stern, and Diego Laplagne for guidance on song playback; Kristin Branson, Alice Robie, Jasper Simon, Michael Dickinson, and the Ctrax community for help with arena design and tracking; and Isabel Gutierrez for expert technical assistance. Marco Gallio, Yuh Nung Jan, Edward Kravitz, Joel Levine, Ernesto Sanchez-Herrero, Julie Simpson, Gerry Rubin, Wesley Grueber, Rebecca Yang, and Bing Zhang provided fly stocks, and Richard Daniels provided the *dVGlut-Gal4* vector. L.B.V. and B.J.D. are investigators of the Howard Hughes Medical Institute.

Received: May 29, 2014
Revised: June 4, 2014
Accepted: June 4, 2014
Published: July 3, 2014

References

1. Dickson, B.J. (2008). Wired for sex: the neurobiology of *Drosophila* mating decisions. Science *322*, 904–909.

2. Yu, J.Y., Kanai, M.I., Demir, E., Jefferis, G.S.X.E., and Dickson, B.J. (2010). Cellular organization of the neural circuit that drives *Drosophila* courtship behavior. Curr. Biol. *20*, 1602–1614.
3. Hall, J.C. (1994). The mating of a fly. Science *264*, 1702–1714.
4. Tompkins, L., and Hall, J.C. (1983). Identification of brain sites controlling female receptivity in mosaics of *Drosophila melanogaster*. Genetics *103*, 179–195.
5. Suzuki, K., Juni, N., and Yamamoto, D. (1997). Enhanced mate refusal in female *Drosophila* induced by a mutation in the *spinster* locus. Appl. Entomol. Zool. (Jpn.) *32*, 235–243.
6. Terhzaz, S., Rosay, P., Goodwin, S.F., and Veenstra, J.A. (2007). The neuropeptide SIFamide modulates sexual behavior in *Drosophila*. Biochem. Biophys. Res. Commun. *352*, 305–310.
7. Sakurai, A., Koganezawa, M., Yasunaga, K.-i., Emoto, K., and Yamamoto, D. (2013). Select interneuron clusters determine female sexual receptivity in *Drosophila*. Nat. Commun. *4*, 1825.
8. Juni, N., and Yamamoto, D. (2009). Genetic analysis of *chaste*, a new mutation of *Drosophila melanogaster* characterized by extremely low female sexual receptivity. J. Neurogenet. *23*, 329–340.
9. Kerr, C., Ringo, J., Dowse, H., and Johnson, E. (1997). *Icebox*, a recessive X-linked mutation in *Drosophila* causing low sexual receptivity. J. Neurogenet. *11*, 213–229.
10. Carhan, A., Allen, F., Armstrong, J.D., Hortsch, M., Goodwin, S.F., and O'Dell, K.M. (2005). Female receptivity phenotype of *icebox* mutants caused by a mutation in the L1-type cell adhesion molecule neuroglian. Genes Brain Behav. *4*, 449–465.
11. Manning, A. (1966). Corpus allatum and sexual receptivity in female *Drosophila melanogaster*. Nature *211*, 1321–1322.
12. Connolly, K., and Cook, R. (1973). Rejection responses by female *Drosophila melanogaster*: Their ontogeny, causality and effects upon the behaviour of the courting male. Behaviour *44*, 142–166.
13. Yapici, N., Kim, Y.J., Ribeiro, C., and Dickson, B.J. (2008). A receptor that mediates the post-mating switch in *Drosophila* reproductive behaviour. Nature *451*, 33–37.
14. Rezával, C., Pavlou, H.J., Dornan, A.J., Chan, Y.B., Kravitz, E.A., and Goodwin, S.F. (2012). Neural circuitry underlying *Drosophila* female postmating behavioral responses. Curr. Biol. *22*, 1155–1165.
15. Yang, C.H., Rumpf, S., Xiang, Y., Gordon, M.D., Song, W., Jan, L.Y., and Jan, Y.-N. (2009). Control of the postmating behavioral switch in *Drosophila* females by internal sensory neurons. Neuron *61*, 519–526.
16. Häsemeyer, M., Yapici, N., Heberlein, U., and Dickson, B.J. (2009). Sensory neurons in the *Drosophila* genital tract regulate female reproductive behavior. Neuron *61*, 511–518.
17. Rezával, C., Nojima, T., Neville, M.C., Lin, A.C., and Goodwin, S.F. (2014). Sexually dimorphic octopaminergic neurons modulate female postmating behaviors in *Drosophila*. Curr. Biol. *24*, 725–730.
18. Ewing, A.W. (1964). The influence of wing area on the courtship behaviour of *Drosophila melanogaster*. Anim. Behav. *12*, 316–320.
19. Crossley, S.A., Bennet-Clark, H.C., and Evert, H.T. (1995). Courtship song components affect male and female *Drosophila* differently. Anim. Behav. *50*, 827–839.
20. Kowalski, S., Aubin, T., and Martin, J.-R. (2004). Courtship song in *Drosophila melanogaster*: a differential effect on male-female locomotor activity. Can. J. Zool. *82*, 1258–1266.
21. von Schilcher, F. (1976). The role of auditory stimuli in the courtship of *Drosophila melanogaster*. Anim. Behav. *24*, 18–26.
22. Dietzl, G., Chen, D., Schnorrer, F., Su, K.C., Barinova, Y., Fellner, M., Gasser, B., Kinsey, K., Oppel, S., Scheiblauer, S., et al. (2007). A genome-wide transgenic RNAi library for conditional gene inactivation in *Drosophila*. Nature *448*, 151–156.
23. Miguel-Aliaga, I., and Thor, S. (2004). Segment-specific prevention of pioneer neuron apoptosis by cell-autonomous, postmitotic *Hox* gene activity. Development *131*, 6093–6105.
24. Celniker, S.E., Keelan, D.J., and Lewis, E.B. (1989). The molecular genetics of the *bithorax* complex of *Drosophila*: characterization of the products of the *Abdominal-B* domain. Genes Dev. *3*, 1424–1436.
25. McGuire, S.E., Mao, Z., and Davis, R.L. (2004). Spatiotemporal gene expression targeting with the TARGET and gene-switch systems in *Drosophila*. Sci. STKE *2004*, pl6.
26. de Navas, L., Foronda, D., Suzanne, M., and Sánchez-Herrero, E. (2006). A simple and efficient method to identify replacements of P-lacZ by P-Gal4 lines allows obtaining Gal4 insertions in the *bithorax* complex of *Drosophila*. Mech. Dev. *123*, 860–867.
27. Lai, S.-L., and Lee, T. (2006). Genetic mosaic with dual binary transcriptional systems in *Drosophila*. Nat. Neurosci. *9*, 703–709.
28. Gordon, M.D., and Scott, K. (2009). Motor control in a *Drosophila* taste circuit. Neuron *61*, 373–384.
29. Estes, P.S., Ho, G.L., Narayanan, R., and Ramaswami, M. (2000). Synaptic localization and restricted diffusion of a *Drosophila* neuronal synaptobrevin—green fluorescent protein chimera in vivo. J. Neurogenet. *13*, 233–255.
30. Wang, J., Ma, X., Yang, J.S., Zheng, X., Zugates, C.T., Lee, C.-H.J., and Lee, T. (2004). Transmembrane/juxtamembrane domain-dependent Dscam distribution and function during mushroom body neuronal morphogenesis. Neuron *43*, 663–672.
31. Kitamoto, T. (2001). Conditional modification of behavior in *Drosophila* by targeted expression of a temperature-sensitive *shibire* allele in defined neurons. J. Neurobiol. *47*, 81–92.
32. Baines, R.A., Uhler, J.P., Thompson, A., Sweeney, S.T., and Bate, M. (2001). Altered electrical properties in *Drosophila* neurons developing without synaptic transmission. J. Neurosci. *21*, 1523–1531.
33. Clyne, J.D., and Miesenböck, G. (2008). Sex-specific control and tuning of the pattern generator for courtship song in *Drosophila*. Cell *133*, 354–363.
34. Daniels, R.W., Gelfand, M.V., Collins, C.A., and DiAntonio, A. (2008). Visualizing glutamatergic cell bodies and synapses in *Drosophila* larval and adult CNS. J. Comp. Neurol. *508*, 131–152.
35. Rideout, E.J., Dornan, A.J., Neville, M.C., Eadie, S., and Goodwin, S.F. (2010). Control of sexual differentiation and behavior by the *doublesex gene* in *Drosophila melanogaster*. Nat. Neurosci. *13*, 458–466.
36. Kvitsiani, D., and Dickson, B.J. (2006). Shared neural circuitry for female and male sexual behaviours in *Drosophila*. Curr. Biol. *16*, R355–R356.
37. Branson, K., Robie, A.A., Bender, J., Perona, P., and Dickinson, M.H. (2009). High-throughput ethomics in large groups of *Drosophila*. Nat. Methods *6*, 451–457.
38. Rybak, F., Sureau, G., and Aubin, T. (2002). Functional coupling of acoustic and chemical signals in the courtship behaviour of the male *Drosophila melanogaster*. P. Roy. Soc. Lond. B Biol. *269*, 695–701.
39. Hamada, F.N., Rosenzweig, M., Kang, K., Pulver, S.R., Ghezzi, A., Jegla, T.J., and Garrity, P.A. (2008). An internal thermal sensor controlling temperature preference in *Drosophila*. Nature *454*, 217–220.
40. Monastirioti, M. (2003). Distinct octopamine cell population residing in the CNS abdominal ganglion controls ovulation in *Drosophila melanogaster*. Dev. Biol. *264*, 38–49.
41. Soller, M., Haussmann, I.U., Hollmann, M., Choffat, Y., White, K., Kubli, E., and Schäfer, M.A. (2006). Sex-peptide-regulated female sexual behavior requires a subset of ascending ventral nerve cord neurons. Curr. Biol. *16*, 1771–1782.
42. Trott, A.R., Donelson, N.C., Griffith, L.C., and Ejima, A. (2012). Song choice is modulated by female movement in *Drosophila* males. PLoS ONE *7*, e46025.
43. Xu, X., Coats, J.K., Yang, C.F., Wang, A., Ahmed, O.M., Alvarado, M., Izumi, T., and Shah, N.M. (2012). Modular genetic control of sexually dimorphic behaviors. Cell *148*, 596–607.
44. Asahina, K., Watanabe, K., Duistermars, B.J., Hoopfer, E., González, C.R., Eyjólfsdóttir, E.A., Perona, P., and Anderson, D.J. (2014). Tachykinin-expressing neurons control male-specific aggressive arousal in *Drosophila*. Cell *156*, 221–235.
45. Pfeiffer, B.D., Ngo, T.-T.B., Hibbard, K.L., Murphy, C., Jenett, A., Truman, J.W., and Rubin, G.M. (2010). Refinement of tools for targeted gene expression in *Drosophila*. Genetics *186*, 735–755.
46. Simon, J.C., and Dickinson, M.H. (2010). A new chamber for studying the behavior of *Drosophila*. PLoS ONE *5*, e8793.
47. Arthur, B.J., Sunayama-Morita, T., Coen, P., Murthy, M., and Stern, D.L. (2013). Multi-channel acoustic recording and automated analysis of *Drosophila* courtship songs. BMC Biol. *11*, 11.

Current Biology, Volume *24*

Supplemental Information

Abdominal-B Neurons Control *Drosophila* Virgin Female Receptivity

Jennifer J. Bussell, Nilay Yapici, Stephen X. Zhang, Barry J. Dickson, and Leslie B. Vosshall

Figure S1

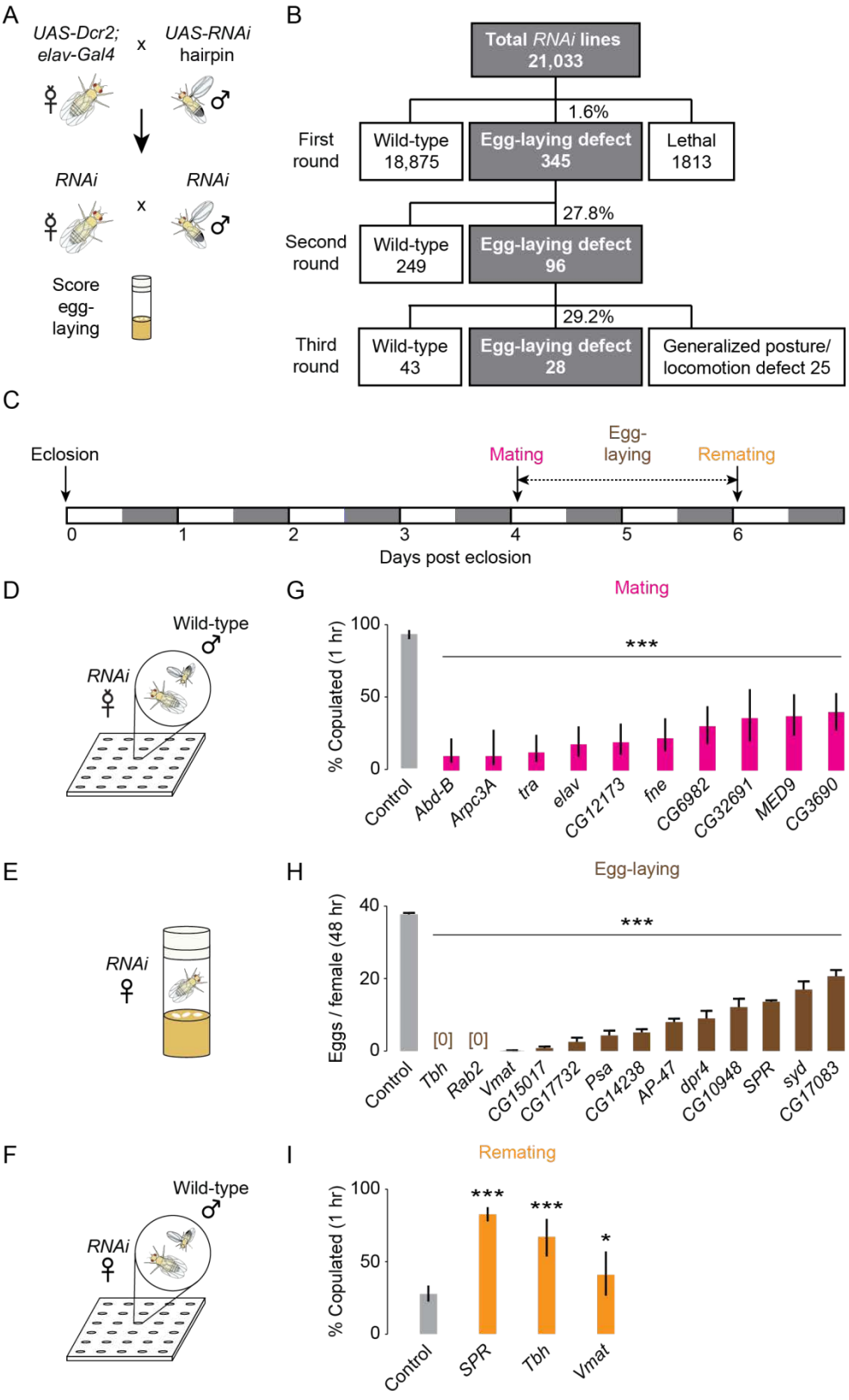
A
UAS-Dcr2; elav-Gal4
x
UAS-RNAi hairpin
RNAi
x
RNAi
Score egg-laying
B
Total RNAi lines 21,033
1.6%
First round
Wild-type 18,875
Egg-laying defect 345
Lethal 1813
27.8%
Second round
Wild-type 249
Egg-laying defect 96
29.2%
Third round
Wild-type 43
Egg-laying defect 28
Generalized posture/ locomotion defect 25
C
Eclosion
Mating
Egg-laying
Remating
0
1
2
3
4
5
6
Days post eclosion
D
Wild-type
RNAi
E
RNAi
F
Wild-type
RNAi
G
Mating
% Copulated (1 hr)
100
50
0
***
Control
Abd-B
Arpc3A
tra
elav
CG12173
fne
CG6982
CG32691
MED9
CG3690
H
Egg-laying
Eggs / female (48 hr)
40
20
0
***
[0]
[0]
Control
Tbh
Rab2
Vmat
CG15017
CG17732
Psa
CG14238
AP-47
dpr4
CG10948
SPR
syd
CG17083
I
Remating
% Copulated (1 hr)
100
50
0
***
***
*
Control
SPR
Tbh
Vmat

Figure S1 (Related to Figure 1). RNAi screen identifies genes required in neurons for female reproductive behaviors. (A) Schematic of crossing scheme and egg-laying assay. (B) Overview of the primary screen. (C) Timeline for secondary assays. (D) Schematic of receptivity assay. (E) Schematic of egg-laying assay. (F) Schematic of remating assay. (G) Receptivity of virgin females with pan-neuronal RNAi targeting the indicated gene paired with single wild-type males (***p <0.001 compared to control, pairwise chi-square test; mean and 95% confidence interval are shown, n = 30-300). (H) Mean number of eggs laid per female during the first 48 h after mating (***p <0.001 compared to control, one-way ANOVA with Sidak correction, mean ± SEM, n = 20–274). (I) Remating frequency (***p <0.001, *p <0.05 compared to control, pairwise chi-square test; mean and 95% confidence interval are shown, n = 44-272).

Figure S2

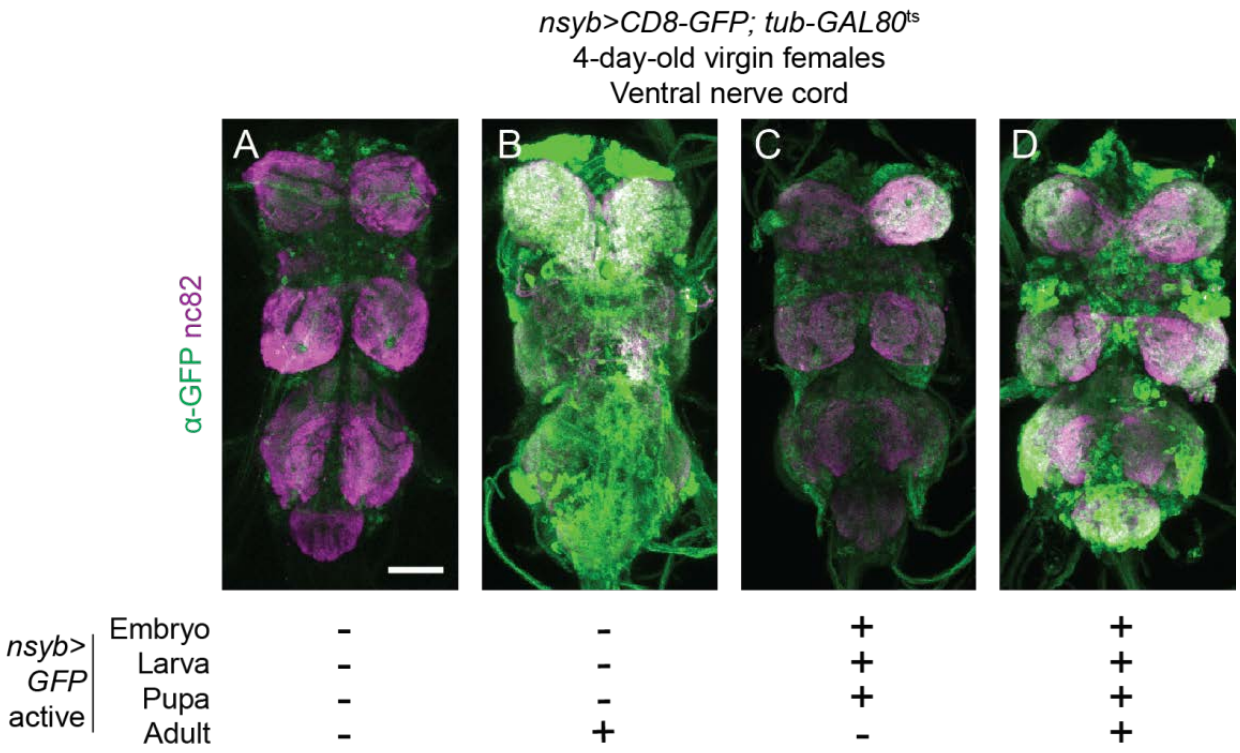

Figure S2 (Related to Figure 1). Effect of *tubGal80*^{ts} induction on nsyb>GFP expression in adult ventral nerve cord. (A-D) Ventral (A, C, D) or dorsal (B) views of ventral nerve cord from females who experienced the following temperature conditions: reared and held at 18°C (A); shifted from 18°C to 30°C at eclosion (B); shifted from 30°C to 18°C at eclosion (C); reared and held at 30°C (D).

Figure S3

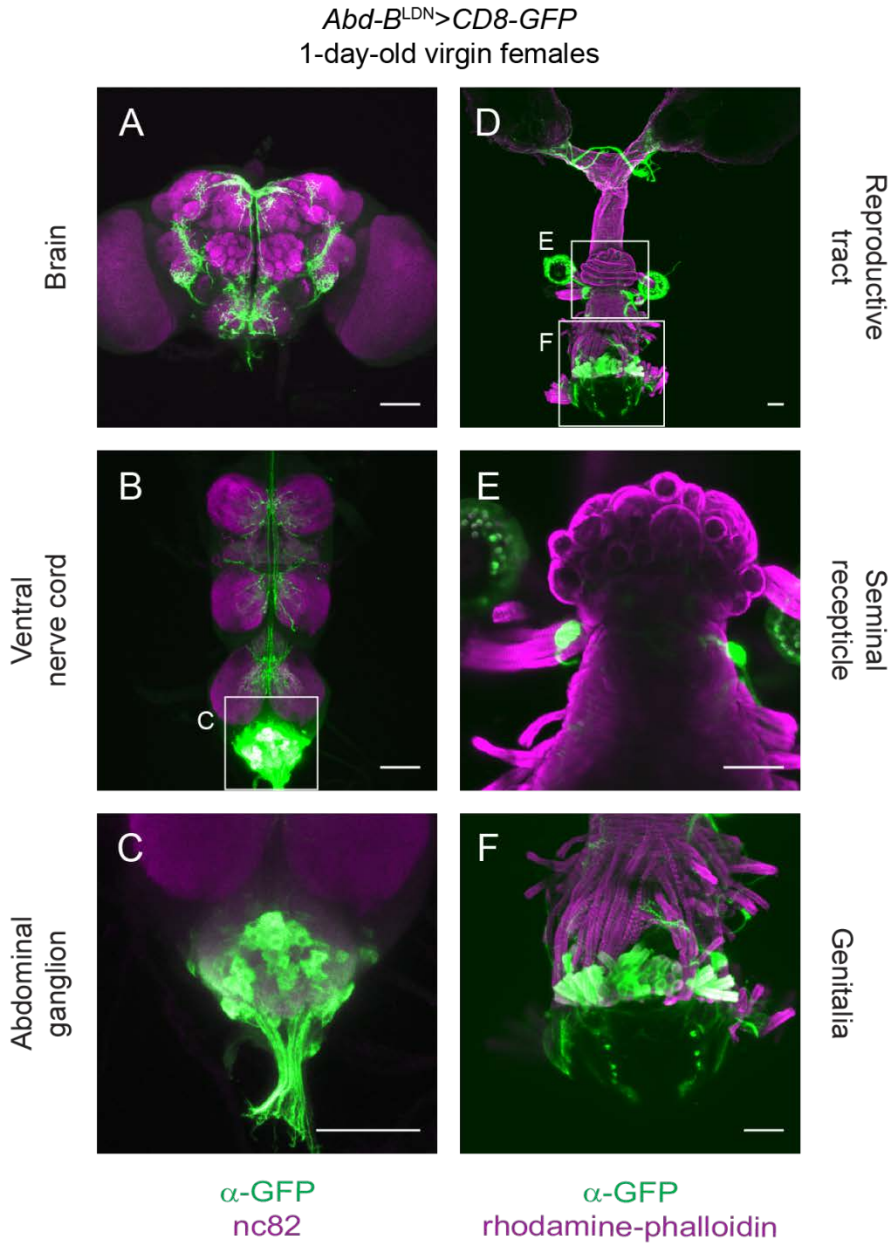

Figure S3 (Related to Figure 3). *Abd-B*^{LDN} neurons in immature virgin females. (A-F) Immunofluorescence of CD8-GFP (green) and nc82 or rhodamine-phalloidin (magenta) in 1-day-old virgin females of the indicated tissues and genotype. Insets in B and D indicate the approximate areas displayed in C, E, and F as separate z-stacks at higher magnification. Scale bars: 50 µm.

Figure S4

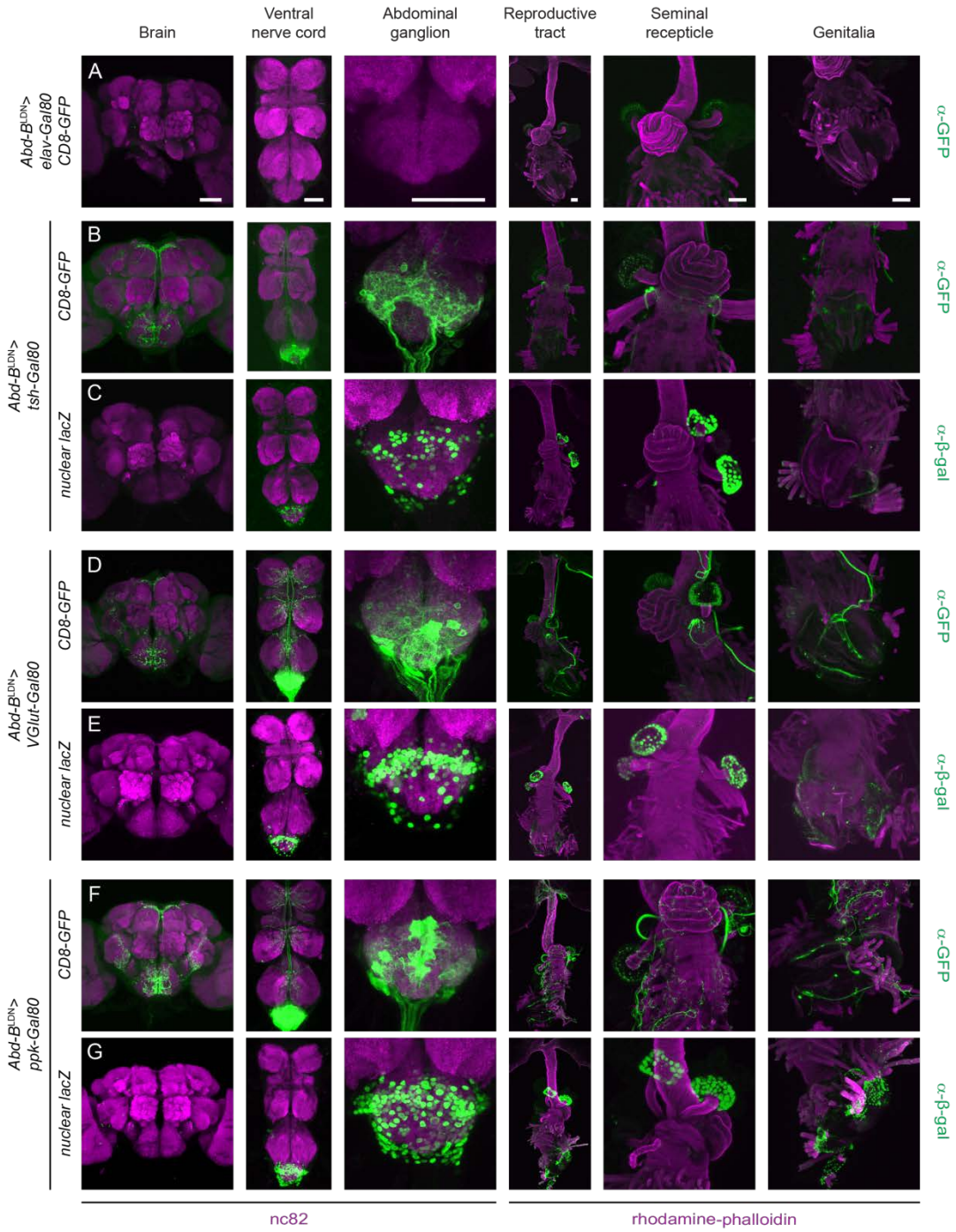

Figure S4 (Related to Figure 4). Repression of *Abd-B*^{LDN}*-Gal4* by various *Gal80* transgenes. (A-G) Immunofluorescence of CD8-GFP or nuclear lacZ (green) and nc82 or rhodamine-phalloidin (magenta) in the indicated tissue in virgin females of the indicated genotype. Scale bars: 50 µm.

Figure S5

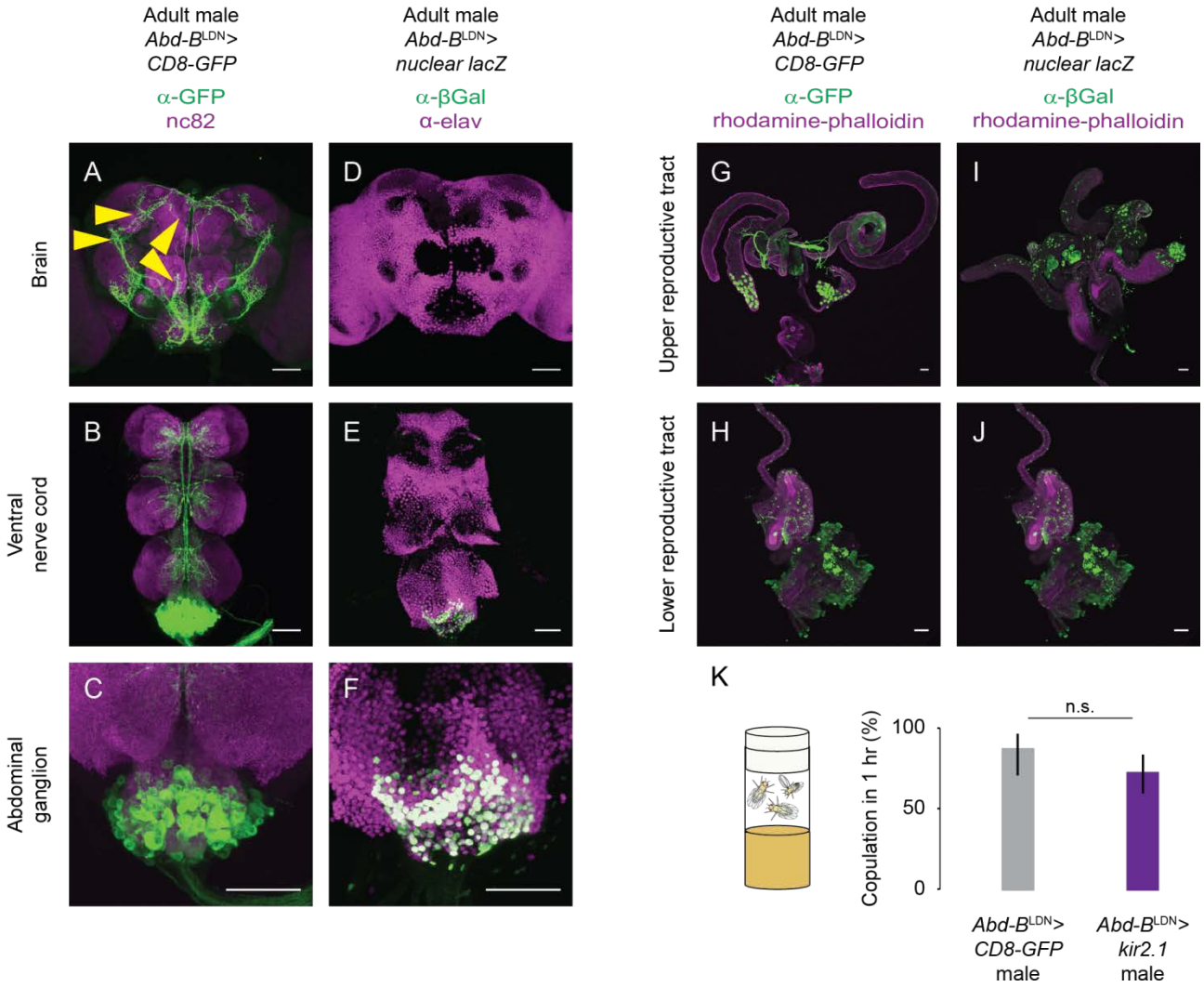

Figure S5 (Related to Figure 4). *Abd-B*^{LDN} neurons in males. (A-J) Immunofluorescence of CD8-GFP or nuclear lacZ (green) and elav or rhodamine-phalloidin (magenta) in the indicated tissues and genotypes. Arrowheads in A indicate potential sites of sexual dimorphism in the brain. Scale bars: 50 µm. (K) Male copulation success (n.s. = not significant, Fisher's exact test. Mean and 95% confidence interval are shown, n = 32-59).

Figure S6

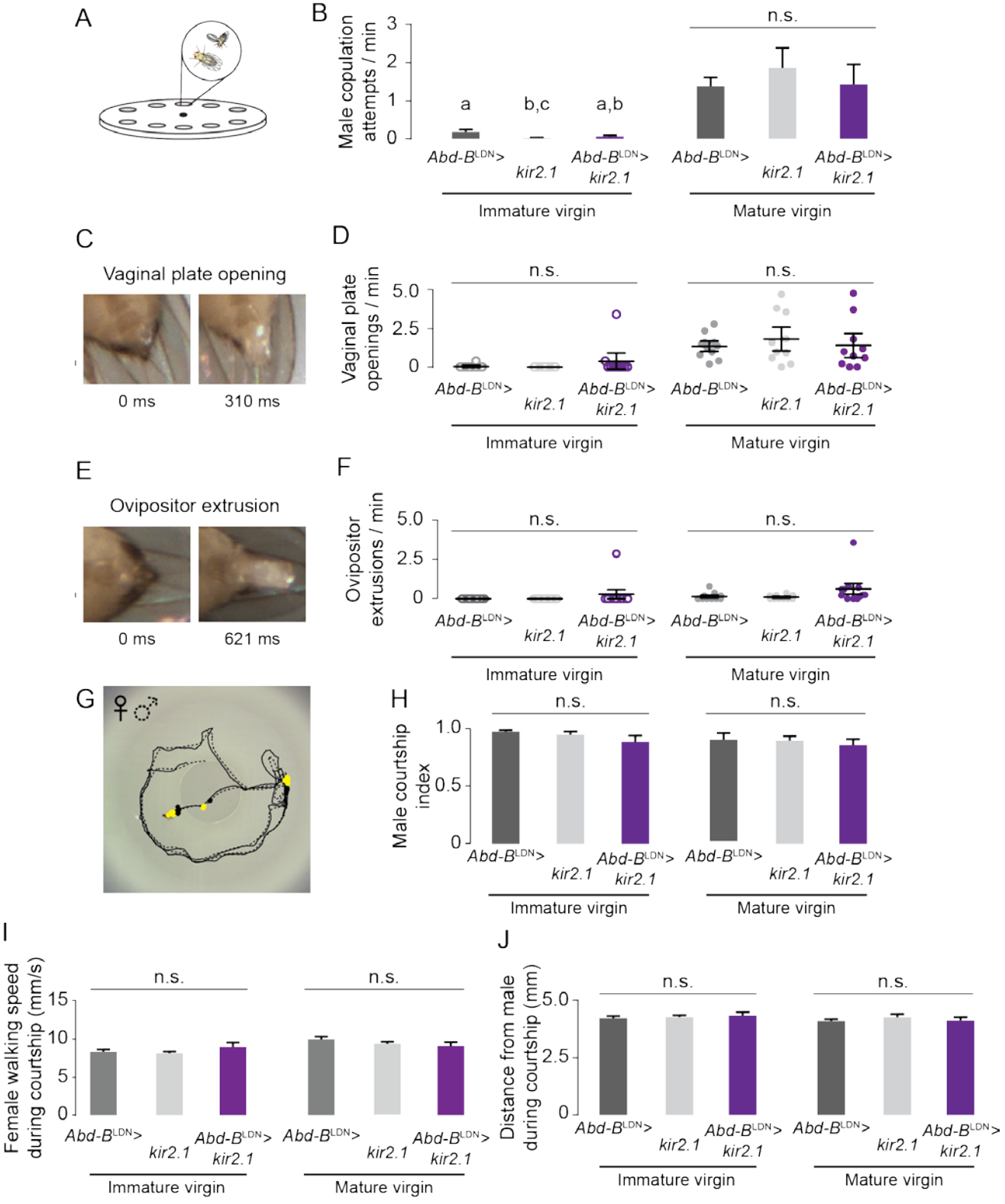
A
B
Male copulation attempts / min
3
2
1
0
a
b,c
a,b
n.s.
Abd-B^LDN>
kir2.1
Abd-B^LDN> kir2.1
Immature virgin
Mature virgin
C
Vaginal plate opening
0 ms
310 ms
D
Vaginal plate openings / min
5.0
2.5
0
n.s.
E
Ovipositor extrusion
0 ms
621 ms
F
Ovipositor extrusions / min
G
H
Male courtship index
1.0
0.5
0
I
Female walking speed during courtship (mm/s)
15
10
5
0
J
Distance from male during courtship (mm)

Figure S6 (Related to Figure 5). Silencing *Abd-B*^{LDN} neurons in females does not affect male courtship behavior or induce female rejection behaviors. (A) Schematic of assay in (B). (B) Male copulation attempts during courtship in 1-cm plastic chambers (Bars labeled with different letters are significantly different, $p < 0.05$; n.s. = not significant, one-way ANOVA with Tukey correction for multiple comparisons, mean ± SEM, n = 10-11). (C, E) Video stills during courtship of vaginal plate opening (C) and ovipositor extrusion 48 h (E) after mating in wild type females. (D, F) Vaginal plate opening (D) and ovipositor extrusion (F) (n.s. = not significant, one-way ANOVA with Bonferroni correction, mean ± SEM, n = 10). (G) Tracking arena with fly positions during the last 60 s before copulation between *Abd-B*^{LDN}*-Gal4* mature virgin female and wild-type male. (H) Male courtship index (n.s. = not significant, one-way ANOVA with Tukey correction for multiple comparisons, mean ± SEM, n = 9-11). (I) Female speed during courtship excluding frames classified as pausing (n.s. = not significant, one-way ANOVA with Tukey correction for multiple comparisons, mean ± SEM, n = 8-10). (J) Female distance from male (n.s. = not significant, one-way ANOVA with Tukey correction for multiple comparisons, mean ± SEM, n = 9-11).

Figure S7

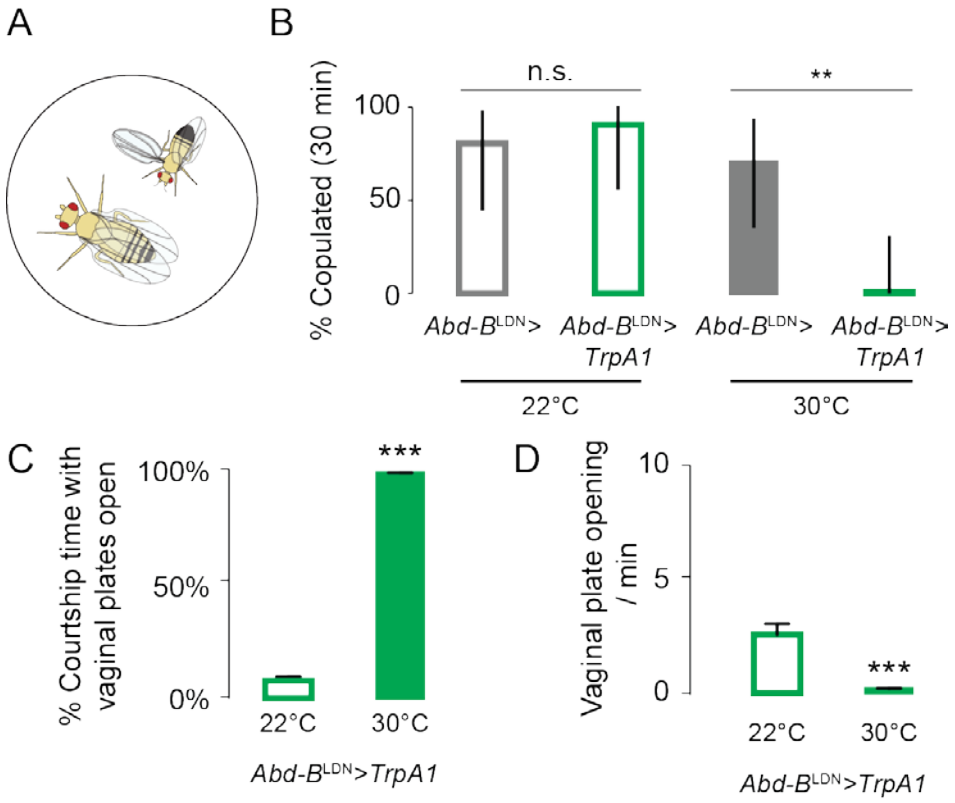

Figure S7 (Related to Figure 7). Activating *Abd-B*^{LDN} neurons locks vaginal plates in the open position, preventing copulation. (A) Schematic of courtship from a wild-type male in tracking arena used in B. (B) Female receptivity at the indicated temperature in tracking arena (**p <0.01, n.s. = not significant, Fisher's exact test. Mean and 95% confidence interval are shown, n = 7-11). (C-D) Time during courtship with vaginal plates open (C) and vaginal plate openings per minute of courtship (D) measured in 1-cm plastic chambers at the indicated temperature (*** p<0.001, Student's t-test, mean ± SEM, n = 5). No ovipositor extrusion was observed in these experiments.

SUPPLEMENTAL EXPERIMENTAL PROCEDURES

Fly Stocks

Virgin females for most crosses were collected using several “virginator” strains, which contain a heat shock-inducible *hid* transgene inserted on the Y chromosome that selectively kills males after 1 h heat shock at 37°C during the pupal stage [S1] [Bloomington *Drosophila* Stock Center (Bloomington) #24638]. Virginator flies themselves were not used in behavior assays. When tested as parental controls, *Gal4* and *UAS* stocks were tested as hemizygotes after crossing to the isogenic w^{1118} strain from the Vienna *Drosophila* RNAi Center (VDRC). All RNAi stocks were obtained from the genome-wide transgenic RNAi library [S2] maintained at the Vienna *Drosophila* RNAi Center (VDRC). The *elav-Gal4* [S3] stock used in the RNAi screen carried a *UAS-Dcr-2* insertion on the X chromosome [S2].

Fly strains and sources are as follows: *nsyb-Gal4* and *tsh-Gal80* (Julie Simpson, HHMI-Janelia Farm Research Campus); *Abd-B*^{LDN}*-Gal4* (Ernesto Sanchez-Herrero, Centro de Biología Molecular Severo Ochoa); *elav-Gal80* (Yuh Nung Jan, UCSF); *nsyb-lexA* and *UAS-shi*^{ts} (Gerry Rubin, HHMI-Janelia Farm Research Campus); *Et*^{FLP250} (Ed Kravitz, Harvard University); *lexAop-FLP* [S4] (Marco Gallio, Northwestern University); *tub-Gal80*^{ts} (Bloomington *Drosophila* Stock Center at Indiana University, stock #7019); *tub-FRT-GAL80-FRT-STOP* (Bing Zhang, University of Missouri); *UAS-nuclear lacZ* (Bloomington #3956; Vanessa Ruta, The Rockefeller University); *UAS-stinger nuclear GFP* (Bloomington #28863; Joel Levine, University of Toronto); *UAS-mCD8-GFP* [S5]; *UAS-nsyb-GFP* (Rami Ramaswami, Trinity College Dublin); *ppk-Gal80* and *UAS-Dscam-GFP* (Wesley Grueber, Columbia University); *UAS-eGFP-kir2.1* (Rebecca Yang, UNC-Chapel Hill), *UAS-TrpA1* (Bloomington #26263). *fru-FLP* was described in [S6].

Virginator strains used to collect virgin females to set crosses: *UAS-Dcr2(x)/hs-hid(y); +; elav-Gal4* (crossed to males from VDRC RNAi library in Figure S1 and Figures 1B and 1D). *UAS-Dcr2(x)/hs-hid(y); +; +* (crossed to males *w; +; nsyb-Gal4/TM3, Sb* and *w; tub-Gal80*^{ts}*; nsyb-Gal4/TM3, Sb*). *UAS-Dcr2(x)/hs-hid(y); +; UAS-Abd-B RNAi* VDRC line

12024/TM3, Sb (crossed to males *w; +; nsyb-Gal4/TM3, Sb* and *w; tub-Gal80^{ts}; nsyb-Gal4/TM3, Sb*). *w (x)/hs-hid(y); +; +* (crossed to males *w; +; UAS-kir2.1-eGFP* and *w; UAS-shi^{ts}; +* and *+; +; UAS-TrpA1*). *w (x)/hs-hid(y); +; Abd-B^{LDN}-Gal4/TM6b* (crossed to males *w; +; UAS-eGFP-kir2.1* and *w; UAS-shi^{ts}; +* and *+; +; UAS-TrpA1* and *w; +; UAS-nlacZ* and *w; +; UAS-mCD8-GFP* and *w; +; UAS-stinger*)

Detailed genotypes of all strains used in the paper are as follows:

Figure 1

Panel B

Females

UAS-Dcr2/w^{1118}; +; elav-Gal4/+
UAS-Dcr2/ w^{1118}; +; elav-Gal4/VDRC RNAi transformant 37915
UAS-Dcr2/ w^{1118}; +; elav-Gal4/VDRC RNAi transformant 46408
UAS-Dcr2/ w^{1118}; VDRC RNAi transformant 26549/+; elav-Gal4/+
UAS-Dcr2/ w^{1118}; +; elav-Gal4/VDRC RNAi transformant 12024
UAS-Dcr2/ w^{1118}; VDRC RNAi transformant 2560/+; elav-Gal4/+
UAS-Dcr2/ w^{1118}; +; elav-Gal4/VDRC RNAi transformant 31674
UAS-Dcr2/ w^{1118}; VDRC RNAi transformant 9673/+; elav-Gal4/+
UAS-Dcr2/ w^{1118}; +; elav-Gal4/VDRC RNAi transformant 41563
UAS-Dcr2/ w^{1118}; +; elav-Gal4/VDRC RNAi transformant 28359
UAS-Dcr2/ w^{1118}; VDRC RNAi transformant 48891/+; elav-Gal4/+

Males

Canton-S wild-type

Panel D

Females

UAS-Dcr2/ w^{1118}; +; elav-Gal4/+
UAS-Dcr2/ w^{1118}; +; nsyb-Gal4/+
w^{1118}; +; VDRC RNAi transformant 12024/+
w^{1118}; VDRC RNAi transformant 104872/+; +
UAS-Dcr2/ w^{1118}; +; elav-Gal4/VDRC RNAi transformant 12024
UAS-Dcr2/ w^{1118}; VDRC RNAi transformant 104872/+; elav-Gal4/+
UAS-Dcr2/ w^{1118}; +; nsyb-Gal4/VDRC RNAi transformant 12024
UAS-Dcr2/ w^{1118}; VDRC RNAi transformant 104872/+; nsyb-Gal4/+

Males

Canton-S wild-type

Panels F-G

Females

UAS-Dcr2/ w^{1118}; +; nsyb-Gal4/+

w^{1118}; +; VDRC RNAi transformant 12024/+
UAS-Dcr2/ w^{1118}; +; nsyb-Gal4/VDRC RNAi transformant 12024

Panel I
UAS-Dcr2/ w^{1118}; tub-Gal80^{ts}/+; nsyb-Gal4/VDRC RNAi transformant 12024

Males
Canton-S wild-type

Figure 2

All panels
Females
UAS-Dcr2/ w^{1118}; +; nsyb-Gal4/+
w^{1118}; +; VDRC RNAi transformant 12024/+
UAS-Dcr2/ w^{1118}; +; nsyb-Gal4/VDRC RNAi transformant 12024

Males
Canton-S wild-type

Figure 3

Panel A
Females
w^{1118}; UAS-nlacZ/+; Abd-B^{LDN}-GAL4/+

Panel B
Females
UAS-Dcr2/tub-FRT-Gal80-FRT-STOP; UAS-CD8-GFP/LexAop-FLP; nsyb-Gal4/nsyb-lexA
UAS-Dcr2/tub-FRT-Gal80-FRT-STOP; UAS-CD8-GFP/LexAop-FLP; nsyb-Gal4/nsyb-lexA, VDRC RNAi transformant 12024

Males
Canton-S wild-type

Panels C-H
Females
w^{1118}; UAS-stinger/+; Abd-B^{LDN}-GAL4/+

Panels I-N
Females
w^{1118}; +; Abd-B^{LDN}-GAL4/UAS-mCD8-GFP

Panels O-T
Females
w^{1118}; +; Abd-B^{LDN}-GAL4/UAS-nsyb-GFP

Panels U-Z

Females

w^{1118}; +; Abd-B^{LDN}-GAL4/UAS-Dscam-GFP

Figure 4

Panels A and B

Females

w^{1118}; +; Abd-B^{LDN}-GAL4/+
w^{1118}; +; UAS-shi^{ts}/+
w^{1118}; +; Abd-B^{LDN}-GAL4/UAS- shi^{ts}

Males

Canton-S wild-type

Panel C

Females

w^{1118}; +; Abd-B^{LDN}-GAL4/+
w^{1118}; +; UAS-eGFP-kir2.1/+
w^{1118}; +; Abd-B^{LDN}-GAL4/ UAS-eGFP-kir2.1
w^{1118}/elav-Gal80; +; Abd-B^{LDN}-GAL4/+
w^{1118}/elav-Gal80; +; Abd-B^{LDN}-GAL4/ UAS-eGFP-kir2.1
w^{1118}; VGlut-Gal80/+; Abd-B^{LDN}-GAL4/+
w^{1118}; VGlut-Gal80/+; Abd-B^{LDN}-GAL4/ UAS-eGFP-kir2.1
w^{1118}; tsh-Gal80/+; Abd-B^{LDN}-GAL4/+
w^{1118}; tsh-Gal80/+; Abd-B^{LDN}-GAL4/ UAS-eGFP-kir2.1
w^{1118}; ppk-Gal80/+; Abd-B^{LDN}-GAL4/+
w^{1118}; ppk-Gal80/+; Abd-B^{LDN}-GAL4/ UAS-eGFP-kir2.1

Males

Canton-S wild-type

Panel D

Females

UAS-STOP-kir2.1/ w^{1118}; +; Abd-B^{LDN}-GAL4/+
w^{1118}; LexAop-FLP/+; nsyb-lexA/+
UAS-STOP-kir2.1/ w^{1118}; LexAop-FLP/+; Abd-B^{LDN}-GAL4/ nsyb-lexA
w^{1118}; ET^{FLP250}/+; +
UAS-STOP-kir2.1/ w^{1118}; ET^{FLP250}/+; Abd-B^{LDN}-GAL4/+
w^{1118}; UAS-STOP-CD8-GFP/+; fru-FLP/+
UAS-STOP-kir2.1/ w^{1118}; UAS-STOP-CD8-GFP/+; Abd-B^{LDN}-GAL4/fru-FLP

Males

Canton-S wild-type

Panels E-J
Females
w^{1118}*; ET*^{FLP250}*/UAS-STOP-CD8GFP; Abd-B*^{LDN}*-GAL4/+*

Panels K-P
Females
w^{1118}*; UAS-STOP-CD8-GFP/+; Abd-B*^{LDN}*-GAL4/fru-FLP*

Figure 5

Panels A, C, E, and F
Females
w^{1118}*; +; Abd-B*^{LDN}*-GAL4/+*

Males
Canton-S wild-type

Panels B and D
Females
w^{1118}*; +; Abd-B*^{LDN}*-GAL4/+*
w^{1118}*; +; UAS-eGFP-kir2.1/+*
w^{1118}*; +; Abd-B*^{LDN}*-GAL4/ UAS-eGFP-kir2.1*

Males
Canton-S wild-type

Figure 6

Panels A, C, and D
Females
w^{1118}*; +; Abd-B*^{LDN}*-GAL4/+*

Males
Canton-S wild-type

Panel E
Females
w^{1118}*; +; Abd-B*^{LDN}*-GAL4/+*
w^{1118}*; +; Abd-B*^{LDN}*-GAL4/ UAS-eGFP-kir2.1*

Males
Canton-S wild-type

Figure 7

Panels B and D
Females
w^{1118}*; +; Abd-B*^{LDN}*-GAL4/+*
w^{1118}*/+; UAS-TrpA1/+; Abd-B*^{LDN}*-GAL4/+*

Males
Canton-S wild-type

Panel E
Female
w^{1118}*; +; Abd-B*^{LDN}*-GAL4/+*

Male
Canton-S wild-type

Panels F and G
Female
w^{1118}*/+; UAS-TrpA1/+; Abd-B*^{LDN}*-GAL4/+*

Male
Canton-S wild-type

Panels I and K
Females
w^{1118}*; +; Abd-B*^{LDN}*-GAL4/+*
w^{1118}*/+; UAS-TrpA1/+; +*
w^{1118}*/+; UAS-TrpA1/+; Abd-B*^{LDN}*-GAL4/+*

Males
Canton-S wild-type

Figure S1

Panel G
Females
UAS-Dcr2/ w^{1118}*; +; elav-Gal4/+*
UAS-Dcr2/ w^{1118}*; +; elav-Gal4/VDRC RNAi transformant 12024*
UAS-Dcr2/ w^{1118}*; VDRC RNAi transformant 26549/+; elav-Gal4/+*
UAS-Dcr2/ w^{1118}*; VDRC RNAi transformant 2560/+; elav-Gal4/+*
UAS-Dcr2/ w^{1118}*; +; elav-Gal4/VDRC RNAi transformant 37915*
UAS-Dcr2/ w^{1118}*; +; elav-Gal4/VDRC RNAi transformant 31674*
UAS-Dcr2/ w^{1118}*; VDRC RNAi transformant 48891/+; elav-Gal4/+*
UAS-Dcr2/ w^{1118}*; VDRC RNAi transformant 9673/+; elav-Gal4/+*
UAS-Dcr2/ w^{1118}*; +; elav-Gal4/VDRC RNAi transformant 46408*
UAS-Dcr2/ w^{1118}*; +; elav-Gal4/VDRC RNAi transformant 41563*
UAS-Dcr2/ w^{1118}*; +; elav-Gal4/VDRC RNAi transformant 28359*

Males
Canton-S wild-type

Panel H

Females

UAS-Dcr2/ w^{1118}; +; elav-Gal4/+
UAS-Dcr2/ w^{1118}; VDRC RNAi transformant 51667/+; elav-Gal4/+
UAS-Dcr2/ w^{1118}; +; elav-Gal4/VDRC RNAi transformant 34767
UAS-Dcr2/ w^{1118}; +; elav-Gal4/VDRC RNAi transformant 4856
UAS-Dcr2/ w^{1118}; VDRC RNAi transformant 47461/+; elav-Gal4/+
UAS-Dcr2/ w^{1118}; VDRC RNAi transformant 40100/+; elav-Gal4/+
UAS-Dcr2/ w^{1118}; VDRC RNAi transformant 35354/+; elav-Gal4/+
UAS-Dcr2/ w^{1118}; VDRC RNAi transformant 2673/+; elav-Gal4/+
UAS-Dcr2/ w^{1118}; +; elav-Gal4/VDRC RNAi transformant 24017
UAS-Dcr2/ w^{1118}; VDRC RNAi transformant 39306/+; elav-Gal4/+
UAS-Dcr2/ w^{1118}; +; elav-Gal4/VDRC RNAi transformant 31388
UAS-Dcr2/ w^{1118}; +; elav-Gal4/VDRC RNAi transformant 7061
UAS-Dcr2/ w^{1118}; +; elav-Gal4/VDRC RNAi transformant 35346
UAS-Dcr2/ w^{1118}; +; elav-Gal4/VDRC RNAi transformant 39936

Males

Canton-S wild-type

Panel I

Females

UAS-Dcr2/ w^{1118}; +; elav-Gal4/+
UAS-Dcr2/ w^{1118}; +; elav-Gal4/VDRC RNAi transformant 7061
UAS-Dcr2/ w^{1118}; VDRC RNAi transformant 51667/+; elav-Gal4/+
UAS-Dcr2/ w^{1118}; +; elav-Gal4/VDRC RNAi transformant 4856

Male

Canton-S wild-type

Figure S2

Panels A-D

Female

w^{1118}/+; tub-Gal80^{ts}/+; nsyb-Gal4/UAS-CD8-GFP

Figure S3

Panels A-F

Females

w^{1118}; +; Abd-B^{LDN}-GAL4/UAS-CD8-GFP

Figure S4

Panel A

Females

w^{1118}/elav-Gal80; +; Abd-B^{LDN}-GAL4/UAS-CD8-GFP

Panel B
Females
w^{1118}; tsh-Gal80/+; Abd-B^{LDN}-GAL4/ UAS-CD8-GFP

Panel C
Females
w^{1118}; tsh-Gal80/+; Abd-B^{LDN}-GAL4/ UAS-nuclear lacZ

Panel D
Females
w^{1118}; VGlut-Gal80/+; Abd-B^{LDN}-GAL4/ UAS-CD8-GFP

Panel E
Females
w^{1118}; VGlut-Gal80/+; Abd-B^{LDN}-GAL4/ UAS-nuclear lacZ

Panel F
Females
w^{1118}; ppk-Gal80/+; Abd-B^{LDN}-GAL4/ UAS-CD8-GFP

Panel G
Females
w^{1118}; ppk-Gal80/+; Abd-B^{LDN}-GAL4/ UAS-nuclear lacZ

Figure S5

Panels A,B,C,G, and H
Males
w^{1118}; +; Abd-B^{LDN}-GAL4/UAS-CD8-GFP

Panels D,E,F, I, and J
Males
w^{1118}; +; Abd-B^{LDN}-GAL4/ UAS-nuclear lacZ

Panel K
Females
Canton-S wild-type

Males
w^{1118}; +; Abd-B^{LDN}-GAL4/UAS-CD8-GFP
w^{1118}; +; Abd-B^{LDN}-GAL4/ UAS-eGFP-kir2.1

Figure S6

Panels B, D, F, H, I, and J
Females
w^{1118}; +; Abd-B^{LDN}-GAL4/+
w^{1118}; +; UAS-eGFP-kir2.1/+

w^{1118}; +; Abd-B^{LDN}-GAL4/ UAS-eGFP-kir2.1

Males
Canton-S wild-type

Panels C and E
Canton-S wild-type

Panel G
Female
w^{1118}; +; Abd-B^{LDN}-GAL4/+

Male
Canton-S wild-type

Figure S7

Panel B
Females
w1118; +; Abd-B^{LDN}-GAL4/+
w1118/+; UAS-TrpA1/+; Abd-B^{LDN}-GAL4/+

Males
Canton-S wild-type

Panels C and D
Females
w1118/+; UAS-TrpA1/+; Abd-B^{LDN}-GAL4/+

Males
Canton-S wild-type

Antibodies

The following antibodies were used at these dilutions and obtained from the listed sources: rabbit anti-GFP (1:2000; catalogue #TP401, Torrey Pines); chicken anti-β-gal (1:2000; Abcam catalogue #9361). The following antibodies were obtained from the Developmental Studies Hybridoma Bank, which was developed under the auspices of the NICHD and maintained by The University of Iowa, Department of Biology, Iowa City, IA 52242: mouse anti-Abd-B (1:50); mouse anti-nc82 (1:10); rat anti-elav (1:100). Secondary fluorescent antibodies were Alexa Fluor 488 Goat anti-Rabbit (1:500; Invitrogen catalogue #11008), Alexa Fluor 488 Goat anti-Chicken (1:500, Invitrogen catalogue #11039); Cy3 Goat Anti-Mouse (1:500; Jackson ImmunoResearch catalogue

#115-165-166), rhodamine-conjugated phalloidin (1:500; Sigma-Aldrich catalogue #P1951).

RNAi screen

Screening: 5-6 females homozygous for both *UAS-Dcr2* on the X chromosome and *elav-Gal4* on the 3rd chromosome were crossed to 3-5 males from a line in the VDRC RNAi library [S2]. Parents were removed from the cross after three days, and progeny were allowed to eclose and were left in the vial for 3-4 days post-eclosion to permit sibling inter-mating. From these vials, 20-30 adult females and 3-5 males were transferred to a fresh food vial where females were allowed to lay eggs for 24 h. The adults were then transferred to a fresh vial and left for another 24 h. Adults were transferred a final time to a fresh vial and females allowed to lay eggs for another 24 h, after which time the adult flies were removed. The number of eggs in each of the three vials was estimated and scored on a 1-5 scale as follows: 1, ~100 or more eggs; 2, ~50-100 eggs; 3, ~20-50 eggs; 4, ~5-20 eggs; 5, ~0-5 eggs. A three-day average score of 3 or more was regarded as positive for decreased egg-laying. Positive RNAi lines were retested twice. If no adults were obtained from a cross, or the majority died before the end of the 3rd day, the RNAi line was scored as lethal.

Phenotype classification: Mating success, egg-laying, and remating success were assayed as outlined in Figure S1C. All assays were performed at ZT6-10, 25°C, 70% relative humidity, and on at least 3 independent occasions. Virgin females were collected at eclosion from crosses of *elav-Gal4* driver line females and RNAi line males. Wild-type males were collected at eclosion and aged individually for 5 days; females were aged for 4 days in groups of 10–15. To determine mating success, single virgin female progeny and wild-type male progeny were paired in 1-cm diameter plastic chambers in a 5 x 5 chamber array and videotaped for 1 h. Those females that copulated were then transferred to single food vials for 48h, and the eggs laid by each female were counted manually. The same females were then re-tested in videotaped pairings with virgin Canton-S males for remating. The data for the *elav-Gal4/+* controls are pooled from separate experiments.

Movement tracking

For each trial, a single female fly was gently aspirated into the arena and allowed to acclimate for 30 s. Then a single male was introduced and recording started. Videos were trimmed to either approximately 30 s after the introduction of the male or courtship initiation, if courtship began fewer than 30 s into the video. Movement was tracked until at least five minutes after courtship initiation or until copulation initiation, depending on female genotype and mating status. Given that an individual female mating decision may not reflect the general receptivity probability of a genotype or mating status, we analyzed trials in which copulation did or did not occur within 15 minutes, as per the normal receptivity of females of that genotype and mating status. Rare trials with fewer than two minutes of courtship were discarded.

Fly speed—the per-frame speed of the fly's center of rotation—is the velmag parameter calculated by the *compute_perframe_stats* script accompanying Ctrax. Frames in which the female paused were identified using a custom Matlab script. Briefly, after manual input of the starting frame of courtship, the script identifies frames where the speed of the female is less than 4 mm/s and her angular acceleration (smoothd2theta in *compute_perframe_stats*) is less than 15 rads/s^2. These values were adjusted to accurately label pauses judged by eye during video playback using the *showtrx* Matlab script accompanying Ctrax. To calculate the fraction of time the female paused during courtship, we determined the video frames in which courtship occurred after its initiation based on the assumption that courtship requires the male following the female. From video playback and manual scoring of courtship indices, we determined that this meant that the male was within a fly-body distance of the female. We therefore labeled all frames after courtship initiation when the center of the male's body was within 10 mm of the center of the female's body as courtship. The percent time paused during courtship is therefore the number of courtship frames when the female paused divided by the total number of courtship frames. A small number of trials in which the female paused more than 30% of courtship time because she was stuck within the sloped side of the chamber were discarded. For females tracked alone, pausing was calculated using the speed, angular acceleration, and pause length criteria for the entire first five minutes following 30 s of acclimation after introduction to the arena.

Sound Playback

Speakers were located 4 cm from the center of the closest chamber and 8 cm from the center from the farthest. Playback intensity was measured for 30 sec of each stimulus in a soundproof chamber using a calibrated microphone (Brüel & Kjaer model 4939) placed just below the mesh bottom of the chamber farthest from the speakers. The mean intensity of the white noise stimulus was 66.3 dB, and the mean intensity of the song stimulus was 70.3 dB, with a mean intensity of pulse song peaks of 85.7 dB. Single male and female pairs or single females were aspirated into each chamber, and the entire wheel was then placed in a humidified incubator (23°C, 60% RH) with backlighting provided by a light board as in above movement tracking experiments. Playback was started and then video recording, followed by movement tracking, was performed as above for 30 min. Female receptivity was calculated from recorded videos. Pause definition parameters were adapted to the smaller chambers: courtship was defined as the center of the male being within 5 mm of the center of the female, and velocity and angular acceleration thresholds were decreased to 2 mm/s and 13 mm/s^2, respectively.

Male copulation success

Single males were gently aspirated into standard fly food vials containing 2 wild-type females at 23^oC. Individual pairs were visually scored for copulation at 5, 10, 15, 30, 45, and 60 minutes to determine the percent copulated during 1 h.

Male copulation attempts

Copulation attempts (Figure S6B), defined as the male curling his abdomen to contact the female, were scored from the same videos used to analyze vaginal plate opening and ovipositor extrusion in Figures S6D and S6F.

Temperature-shifted vaginal plate opening and ovipositor extrusion

Assays were carried out as described for Figures S6D and S6F, except that a 1-cm circular plastic chamber was placed on white paper in a heated slide mount attached to a temperature controller (Warner Instruments CL-10), and the mount was placed on top

of a cooling block (BioQuip 1424). A probe just underneath the chamber was used to monitor the temperature, and flies were introduced after the chamber reached the appropriate temperature. Plate opening was scored blind to assay temperature.

SUPPLEMENTAL REFERENCES

S1. Starz-Gaiano, M., Cho, N.K., Forbes, A., and Lehmann, R. (2001). Spatially restricted activity of a *Drosophila* lipid phosphatase guides migrating germ cells. Development *128*, 983-991.

S2. Dietzl, G., Chen, D., Schnorrer, F., Su, K.C., Barinova, Y., Fellner, M., Gasser, B., Kinsey, K., Oppel, S., Scheiblauer, S*., et al.* (2007). A genome-wide transgenic RNAi library for conditional gene inactivation in *Drosophila*. Nature *448*, 151-156.

S3. Luo, L., Liao, Y.J., Jan, L.Y., and Jan, Y.N. (1994). Distinct morphogenetic functions of similar small GTPases: *Drosophila* Drac1 is involved in axonal outgrowth and myoblast fusion. Genes Dev. *8*, 1787-1802.

S4. Shang, Y., Griffith, L.C., and Rosbash, M. (2008). Light-arousal and circadian photoreception circuits intersect at the large PDF cells of the *Drosophila* brain. Proc. Natl. Acad. Sci. USA *105*, 19587-19594.

S5. Lee, T., and Luo, L. (1999). Mosaic analysis with a repressible cell marker for studies of gene function in neuronal morphogenesis. Neuron *22*, 451-461.

S6. Yu, J.Y., Kanai, M.I., Demir, E., Jefferis, G.S.X.E., and Dickson, B.J. (2010). Cellular organization of the neural circuit that drives *Drosophila* courtship behavior. Curr. Biol. *20*, 1602-1614.